

Review

# Lanthanide Oxides in Ammonia Synthesis Catalysts: A Comprehensive Review

Wojciech Patkowski \*, Magdalena Zybert , Hubert Ronduda and Wioletta Raróg-Pilecka \*

Faculty of Chemistry, Warsaw University of Technology, Noakowskiego 3, 00-664 Warsaw, Poland; magdalena.zybert@pw.edu.pl (M.Z.); hubert.ronduda@pw.edu.pl (H.R.)

\* Correspondence: wojciech.patkowski@pw.edu.pl (W.P.); wioletta.pilecka@pw.edu.pl (W.R.-P.)

**Abstract:** The production of ammonia through the Haber–Bosch process is a large-scale catalytic industrial endeavour with substantial energy consumption. A key area of energy optimisation for this process involves efforts to ease the synthesis reaction conditions, particularly by reducing the operating pressure. To achieve this goal, new catalysts are designed to function effectively at lower pressures and temperatures. In recent years, reports in the literature concerning including lanthanide oxides in the catalysts' composition have started appearing more frequently. This review article offers a concise overview of the pivotal role that lanthanide oxides play in the field of ammonia synthesis catalysts. The paper delves into the diverse utilisation of lanthanide oxides, emphasising their role in catalytic systems. The review explores recent advances in the design of catalysts incorporating lanthanide oxides as promoters or support materials, highlighting their impact on enhancing catalyst stability, activity, and operation. Three main groups of catalysts are discussed, where iron, ruthenium, and cobalt constitute the active phase. Insights from recent research efforts are synthesised to provide a comprehensive perspective on the application prospects of lanthanide oxides in ammonia synthesis catalysts.

**Keywords:** ammonia synthesis; lanthanide oxides; iron catalyst; ruthenium catalyst; cobalt catalyst



**Citation:** Patkowski, W.; Zybert, M.; Ronduda, H.; Raróg-Pilecka, W. Lanthanide Oxides in Ammonia Synthesis Catalysts: A Comprehensive Review. *Catalysts* **2023**, *13*, 1464. <https://doi.org/10.3390/catal13121464>

Academic Editor: Concetta Ruocco

Received: 31 October 2023

Revised: 21 November 2023

Accepted: 22 November 2023

Published: 23 November 2023



**Copyright:** © 2023 by the authors. Licensee MDPI, Basel, Switzerland. This article is an open access article distributed under the terms and conditions of the Creative Commons Attribution (CC BY) license (<https://creativecommons.org/licenses/by/4.0/>).

## 1. Introduction

Large-scale ammonia production is carried out via the catalytic Haber–Bosch process. An industrial plant may require more than 450 °C and more than 20 MPa of pressure to run efficiently [1]. Demanding reaction conditions, in addition to the reagents being obtained from fossil fuel processing, cause the process to consume more than 1.5% of the annual energy production and emit 1.9 tonnes of CO<sub>2</sub> per tonne of ammonia produced [2]. It is then crucial to develop novel catalytic systems or re-engineer existing ones to enable more sustainable ammonia production at milder conditions to be suitable for a hydrogen-driven economy.

Nowadays, researchers focus on creating catalytic systems based on transition metals other than iron, such as ruthenium or cobalt, because conventional systems are already considered mature technology with limited possibilities for performance improvement. In the case of transition metal-based catalysts, support is often opted for to obtain high metal dispersion, use the metal particle surface as efficiently as possible, and decrease the loading of costly metals of limited supply. Since the support can also be the functional component of the catalytic system, its selection should not be arbitrary. The material must provide proper stability to the catalyst and sufficiently enhance its performance in the reaction by modifying the active phase properties.

Ammonia synthesis catalyst activity benefits greatly from additives that increase the active surface's basicity. When the basicity and electron-donating capabilities of the catalyst surface increase, the weakening of the dinitrogen bond is facilitated [3]. It is established that increasing the electron density of occupied states near the Fermi level on the metal

atoms is necessary to increase the rate of nitrogen adsorption and dissociation [4]. Then, the excessive electrons located at the d-band can be donated to the  $\pi^*$  antibonding states of the adsorbate [5]. This weakens the triple bond in its molecule, facilitates its dissociation, and accelerates the rate-limiting step of ammonia synthesis [6].

In this context, lanthanide oxides are very frequently used as catalyst supports, promoters, or other modifying elements [7–9] due to their rich chemistry and abundance of beneficial properties in terms of the ammonia synthesis reaction. This review was prepared to gain a perspective on what has already been accomplished in the field, provide a roadmap of conducted research, and direct the prospects of future studies regarding applying lanthanide oxides in ammonia synthesis catalysts. Even though several other reviews aiming to present the application of lanthanide oxides in catalytic systems have been published in recent years [10–12], they tend to focus primarily on ruthenium catalysts as research on this topic is most abundant, and these systems usually display the highest activity. However, we feel that not enough attention is paid to cobalt-based catalysts since numerous papers have recently been published on this topic, revealing many interesting phenomena. Therefore, this paper aims to address this issue and elaborate on this topic. We first discuss the properties of lanthanide oxides, focusing on those that are crucial for the efficient operation of  $\text{NH}_3$  synthesis catalysts. Next, we present and discuss the literature that reports using lanthanide oxides as promoters or supports of three main modern groups of  $\text{NH}_3$  synthesis catalysts: iron-, ruthenium-, and cobalt-based.

Despite the extended study of intellectual property rights in the area of lanthanide oxide utilisation in ammonia synthesis catalysts being different from the aim of this study, it is worth noting that a number of the presented studies resulted in patents. This indicates that the related research was often planned and conducted with industrial application in mind. While the phenomena or general characteristics of catalysts are published in papers, the detailed methods of the synthesis, compositions, and applications of catalysts are most often proprietary, especially in the case of prospective systems with remarkable properties. Some examples of such patents concerning certain catalyst types, created due to the work of particular research groups, are indicated in this review. Notably, the number of patents for novel systems is systematically growing [13]. CASALE SA, Fuzhou University, ThyssenKrupp AG, and Haldor Topsøe own most patents among different entities.

## 2. Lanthanides, Lanthanide Oxides, and Their Properties

Lanthanide oxides derive from bastnasite, monazite, and xenotime ores, minerals that contain phosphates and carbonates of rare-earth metals [14]. They are obtained through a multi-stage process: the physical treatment of the ore, beneficiation, hydrometallurgical or pyrometallurgical processes (calcination), and finally, the separation of individual oxides [15,16]. Lanthanide oxides are in the form of white or light-coloured solids. They all display a relatively small specific surface area (a few to several dozen  $\text{m}^2 \text{g}^{-1}$ ) and high melting points exceeding 2000 °C [17]. They are widely used in ceramics (pigments and glasses), optical applications (lasers), electronics, nuclear power (control rods) industries, and catalysis [17,18].

Lanthanides, as a group, exhibit similar physicochemical properties. From a chemical point of view, these elements are characterised by a gradual variation in the electron configuration (filling of the 4f orbital) resulting from their location in the periodic table. Therefore, lanthanides exhibit certain regularly variable atomic features that determine the chemical properties and structure of the compounds they form, including oxides. One of the fundamental parameters is the ionic radius of a given element's atom (cation). In the case of lanthanides, the phenomenon called lanthanide contraction is observed [19]: a decrease in the atomic or ionic radius that is gradual but more significant than would result from the predictions of periodic trends [20,21]. As the atomic numbers of lanthanides increase, so does the number of electrons on the 4f subshell. Relative to the electrons located on subshells closer to the nucleus, their shielding effect on the remaining electrons is weakened. Consequently, the electrons at the lower subshells are attracted more strongly

by the increasing positive charge of the nucleus. As a result, the given lanthanide's ionic (and atomic) radius decreases.

Table 1 presents selected atomic properties of lanthanides. As indicated by the ionisation energies and electron configuration, the occurrence of the  $\text{Ln}^{3+}$  cation is characteristic of all lanthanides. This cation exhibits high stability, causing  $\text{Ln}_2\text{O}_3$  sesquioxide to be the most common system. However, it is worth noting that three elements display lower fourth ionisation potential compared to the other lanthanides. These are Ce, Pr, and Tb; in their case, a stable cation on the +4 oxidation state is also very common. As a result, they can also exhibit more complex stoichiometry, dependent on the  $\text{Ln}^{3+}/\text{Ln}^{4+}$  ratio, usually with an oxygen deficit in the structure. These are described by the  $\text{Ln}_n\text{O}_{2n-2m}$  formula, where  $n = 1$  to  $\infty$ , and  $m = 1$  to 8. The stable structures for the given three elements, existing under normal conditions, are  $\text{CeO}_2$ ,  $\text{Pr}_6\text{O}_{11}$ , and  $\text{Tb}_4\text{O}_7$ , and some metastability is also demonstrated by the  $\text{PrO}_2$  and  $\text{TbO}_2$  [22,23]. However, these structures may alter their stoichiometry due to the temperature or partial pressure of oxygen changes in the environment [24,25].

**Table 1.** Selected properties of rare-earth elements. Reproduced with permission from ref. [26]. © Springer Nature 2004.

Element	Electronic Configuration	A Sum of the First Three Ionisation Potentials [ $\text{kJ mol}^{-1}$ ]	Fourth Ionisation Potential [ $\text{kJ mol}^{-1}$ ]	$\text{Ln}^{3+}$ Ionic Radius [pm] [27,28]
La	$5d^1 6s^2$	3455	4819	117
Ce	$4f^1 5d^1 6s^2$	3523	3547	115
Pr	$4f^3 6s^2$	3627	3761	113
Nd	$4f^4 6s^2$	3697	3899	112
Pm	$4f^5 6s^2$	3740	3966	111
Sm	$4f^6 6s^2$	3869	3994	110
Eu	$4f^7 6s^2$	4036	4110	109
Gd	$4f^7 5d^1 6s^2$	3749	4245	108
Tb	$4f^9 6s^2$	3791	3839	106
Dy	$4f^{10} 6s^2$	3911	4001	105
Ho	$4f^{11} 6s^2$	3924	4101	104
Er	$4f^{12} 6s^2$	3934	4115	103
Tm	$4f^{13} 6s^2$	4045	4119	102
Yb	$4f^{14} 6s^2$	4194	4220	101
Lu	$4f^{14} 5d^1 6s^2$	3887	4360	100

The atomic properties of lanthanides presented in Table 1 also affect the crystal structure of the oxides they form. This is due to the changes in electron configuration. The variation concerns the 4f orbital, which, due to its location, is relatively well shielded from the influence of the chemical environment by the outer electron shell ( $5s^2p^6$ ). This organisation of the electronic structure weakens the crystal field splitting effects [29] and reduces the covalent bond contribution in the crystal lattice. As a result, the proportion of ionic bonds and electrostatic interactions in the formation of crystals increases [30], together with the contribution of the ionic radius of the lanthanide cation. Consequently, rare-earth oxides exhibit polymorphism and can exist in various crystalline structures. However, some structures are more energy-sustainable and, thus, more common.

Five varieties of polymorphic oxides with  $\text{Ln}_2\text{O}_3$  stoichiometry have been distinguished in the literature as A, B, C, H, and X types. The first three types, A, B, and C, occur at standard conditions. The last two types, H and X, are found stable only at temperatures above 2000 °C [31]; therefore, they will not be discussed in detail. The polymorphic type in which the oxides occur depends on the ionic radius, their synthesis method, and the temperatures and atmospheres or subsequent thermal treatment used [32].

Type A is a hexagonal system of the  $P\bar{3}2m1$  space group [33]. The  $\text{Ln}^{3+}$  cation is bound to seven oxide anions, whereby six  $\text{O}^{2-}$  anions form an octahedron, and the remaining

$O^{2-}$  is located on one of its sides.  $La_2O_3$  and  $Nd_2O_3$  exhibit this structure. Type B is a monoclinic system with type A distortion. It is of the  $C2/m$  space group [34,35]. The metal cations in this structure have a coordination number of six or seven. As in type A, six  $O^{2-}$  anions form an octahedron, but the seventh anion is slightly farther from the cation. Under standard conditions, oxides ranging from  $Nd_2O_3$  to  $Dy_2O_3$  can exhibit this transitional structure, although they will slowly morph into type C. It is a cubic system, of the  $Ia\bar{3}$  space group, with a bixbyite structure [36]. The  $Ln^{3+}$  cation forms six coordination bonds with oxide anions. The unit cell consists of 32 metal cations and 48 oxide anions with a double fluorite structure with every fourth  $O^{2-}$  anion missing. The C-type structure is exhibited by oxides from  $Pr_2O_3$  to  $Lu_2O_3$ . The fluorite structure is exhibited by oxides with  $LnO_2$  stoichiometry, organised into a  $Fm\bar{3}m$  space group [26]. It is a face-centred cubic structure in which the lattice is formed by a  $Ln^{4+}$  cation coordinated with eight  $O^{2-}$  anions, located in tetrahedral space, where each anion connects with another four cations. In this structure, a lanthanide may also occur at the +3 oxidation state, but the change in valence occurs due to the generation and disappearance of oxygen vacancies in the structure. This structure is demonstrated by  $CeO_2$  and adequately defective  $Pr_6O_{11}$  and  $Tb_4O_7$  [31].

The lanthanide oxide's electronic and crystal structure will influence its properties. One of the most important factors for the effective operation of an ammonia synthesis catalyst is the basicity of its surface. The ability to donate electrons (according to Lewis's definition) is crucial as it facilitates the dissociation of adsorbed gas molecules. As the bonds in the crystal lattice of oxides are about 75% ionic (which results from the electronegativity of the elements forming them), lanthanide oxides are basic oxides, and their basicity is comparable to that of alkali metal oxides [32]. Hence, the gradual decrease in the ionic radius of lanthanide cations and ionic charge density [37] progressing along the period from  $La^{3+}$  to  $Lu^{3+}$  will result in a fairly smooth change, i.e., a decrease in basicity [38].

One of the material surface basicity estimating methods, which accounts for the power and number of basic sites of the Lewis type, is the measurement of the adsorption capacity of a gas molecule with acidic properties, e.g.,  $CO_2$  [39]. The basicity of lanthanide oxides was investigated by Sato et al. [40]. Results of the study are presented in Figure 1.

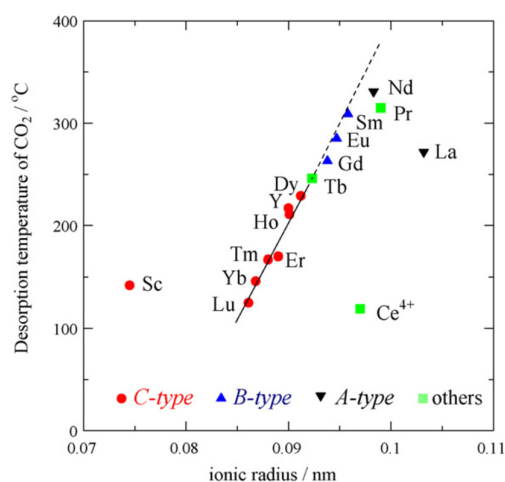


**Figure 1.** Relationship between the radius of rare-earth cation and strength of basic sites of REOs calcined at 1000 °C. The strength of basic sites is defined as the temperature of the  $CO_2$  desorption peak observed below 500 °C. Reproduced with permission from ref. [40]. © Elsevier 2009.

Sato's research indicated a direct correlation between the ionic radius of the lanthanide  $Ln^{3+}$  cation and the strength of the basic sites on the oxide surface. A certain degree of deviation from the linear relationship in the case of some of the lanthanides ( $La_2O_3$  and  $Nd_2O_3$ ) was explained by the different crystal structures they tend to display (type A, hexagonal) and the formation of surface carbonates in contact with carbon dioxide in air. Sato also demonstrated the relationship between the decrease in the total number of basic

sites and their increasing concentration on the surface with the decrease in the ionic radius of the  $\text{Ln}^{3+}$  cation [40,41].

Surface carbonate stability testing can also assess the basicity of lanthanide oxides. Maitra et al. used this method in their research [42]. As a determinant of the basicity of the oxide, the last stage of surface carbonate decomposition temperature was assumed. The series of decreasing basicity estimated by the author was as follows:  $\text{La} > \text{Pr} \sim \text{Nd} > \text{Sm} > \text{Gd} \sim \text{Eu} > \text{Tb} \sim \text{Ho} \sim \text{Er} > \text{Dy} \sim \text{Tm} \sim \text{Yb} \sim \text{Lu} > \text{Ce}$ . Despite the general agreement of the series with the one resulting from predictions based on the electronic structure of cations, Maitra pointed out the difficulty of obtaining consistent results using this method. As causes, he indicated the possible influence of impurities present in oxides, the influence of polymorphism on the structure and temperature of carbonate decomposition, the narrow span of temperatures at which the decomposition reaction occurs, and the dependence of the reaction progress on the composition of gaseous atmosphere.

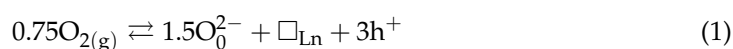
In addition to the electron donation capability of lanthanide oxide surfaces, their ability to transport electrons in bulk, i.e., conductivity, is also worth discussing. The parameters describing the conductivity of lanthanide oxides are presented in Table 2.

**Table 2.** Electrical conductivity data of rare-earth sesquioxides for  $p_{\text{O}_2} = 0.02$  MPa. Reproduced with permission from ref. [43]. © Elsevier 1970.

Lanthanide Oxide	$T_B$ [°C]	$E_1$ ( $T < T_B$ ) [eV]	$E_2$ ( $T > T_B$ ) [eV]	$\sigma$ 400 °C [ $\times 10^9 \Omega^{-1} \text{cm}^{-1}$ ]	$\sigma$ 650 °C [ $\times 10^9 \Omega^{-1} \text{cm}^{-1}$ ]
$\text{La}_2\text{O}_3$	270	0.7	1.05	230	1700
$\text{Pr}_2\text{O}_3$	320	0.4	0.95	300	3450
$\text{Nd}_2\text{O}_3$	-	-	1.15	25	1450
$\text{Sm}_2\text{O}_3$	560	0.6	1.28	20	880
$\text{Eu}_2\text{O}_3$	570	0.6	1.35	5	150
$\text{Gd}_2\text{O}_3$	560	0.5	1.57	5	130
$\text{Tb}_2\text{O}_3$	280	0.4	0.95	3	200
$\text{Ho}_2\text{O}_3$	575	0.7	1.61	5	160
$\text{Yb}_2\text{O}_3$	605	0.5	1.61	3	50

$T_B$ —the breakpoint at which for the  $\log \sigma = f(1/T)$  function, a change in the activation energy of the lanthanide oxides conductivity occurs;  $E_1$  ( $T < T_B$ )—the activation energy of the conduction of a substance at temperatures below the  $T_B$ ;  $E_2$  ( $T > T_B$ )—conductivity activation energy of a substance at temperatures above the  $T_B$ ;  $\sigma$  400 °C, 650 °C—specific conductivity of the substance at 400 °C and 650 °C.

The conductivity of oxides with the  $\text{Ln}_2\text{O}_3$  stoichiometry is relatively low, although variable. The electrical conductivity of oxides depends on the radius of the  $\text{Ln}^{3+}$  cation and increases as it increases. As the temperature increases, the conductivity of all oxides increases linearly, and above the break temperature  $T_B$ , the rate of increase in conductivity rises. The break temperature also varies between oxides and increases with the atomic number of lanthanides. With it, the  $E_2$  conduction activation energy (above the  $T_B$  temperature), necessary for the electron to jump from the valence band to the conduction band, also increases. Lanthanide oxides can be considered mixed conductors; as the ionic component has a certain share in conductivity, the electronic one is mainly responsible for material conductivity [43]. Under standard conditions,  $\text{Ln}_2\text{O}_3$  oxides exhibit p-type conductivity [44]. The holes formed along with the cationic vacancies due to the penetration of oxygen into the crystal lattice of the oxide are responsible for the transfer of charges, according to Equation (1):



where  $\text{O}_0^{2-}$  is an oxide anion at the node of the crystal lattice,  $\square_{\text{Ln}}$  is a cationic vacancy, and  $\text{h}^+$  is a hole.

As the partial pressure of oxygen decreases, the p-type conductivity decrease is observed, while the n-type conductivity increases due to the elimination of oxygen from the crystal lattice and the formation of oxygen vacancies, according to Equation (2):



where  $\square_{\text{O}}$  is an anionic vacancy, and  $\text{e}^-$  is a free electron.

The share of n-type conductivity is higher in oxides with a higher number of  $\text{Ln}^{4+}$  cations in the lattice and for those that exhibit oxygen defects in their structure (or a tendency to form them), i.e.,  $\text{CeO}_2$  or Pr and Tb oxides [43,45].

### 3. Iron-Based Catalysts

Reports on using lanthanide oxides in modifying iron catalysts are few. However, the available literature sheds some light on the effects the modification induces on the performance of the iron catalyst. The reports concern the conventional fused iron-based system. Aleksic et al. [46] investigated samarium oxide as a structural promoter and demonstrated its effect on the porosity of a reduced iron catalyst. The contact promoted with  $\text{K}_2\text{O}$  and  $\text{Sm}_2\text{O}_3$  displayed pores with a larger average dimension of 70 nm, compared to the reference catalyst (containing  $\text{K}_2\text{O}$  and  $\text{Al}_2\text{O}_3$ ) with a pore diameter of 40 nm. The structural effect of  $\text{Sm}_2\text{O}_3$  on surface development and porosity increase in fused iron catalysts was also demonstrated in other studies, again by Aleksic et al. [47] and Mitov et al. [48]. A beneficial effect on the catalyst reduction rate was also confirmed for  $\text{Sm}_2\text{O}_3$ . However, it was accompanied by a slight increase in the reaction activation energy. Berengarten et al. [49] investigated a double-promoted iron catalyst with  $\text{K}_2\text{O}$  in different loadings and a selected structural promoter:  $\text{Al}_2\text{O}_3$ ,  $\text{Ho}_2\text{O}_3$ ,  $\text{Dy}_2\text{O}_3$ , or  $\text{Er}_2\text{O}_3$ . He demonstrated lanthanide oxides' structural effect and contribution to increasing the second electronic promoter performance. The influence of  $\text{K}_2\text{O}$  is stronger in their presence than in the case of the reference system promoted with  $\text{Al}_2\text{O}_3$ . It leads to an increase in the activity and a decrease in the work function of electrons from the iron surface. Other reports also indicated that introducing  $\text{Eu}_2\text{O}_3$  [50] or  $\text{CeO}_2$  [50–54] develops the surface area and increases the porosity of the reduced iron catalyst.

Studies conducted by Karaslavova et al. [55], concerning yttrium oxides, and by Zakieva et al. [56], focusing on the addition of  $\text{Er}_2\text{O}_3$ ,  $\text{La}_2\text{O}_3$ ,  $\text{Pr}_2\text{O}_3$ , and  $\text{Sc}_2\text{O}_3$  instead of  $\text{Al}_2\text{O}_3$ , also confirmed the pro-structural action of lanthanide oxides and the facilitation, i.e., decrease, of the temperature of catalyst reduction. It was demonstrated that the increasing influence of the oxide was correlated with the decrease in the lanthanide cation radius.

Yu et al. [57] investigated the properties of a multi-promoted iron catalyst ( $\text{K}_2\text{O}$ ,  $\text{Al}_2\text{O}_3$ , and  $\text{CaO}$ ) with the addition of a rare-earth gangue, being a mixture of lanthanide oxides such as  $\text{La}_2\text{O}_3$ ,  $\text{CeO}_2$ ,  $\text{Pr}_6\text{O}_{11}$ , and  $\text{Nd}_2\text{O}_3$ . The catalysts were compared with lanthanide-free reference catalysts and an industrial cobalt-containing fused iron system (ICI74-1). The catalyst obtained by melting magnetite ore, promoter precursors, and gangue reduced to a greater extent and at a lower temperature than the reference catalysts. Additionally, the gangue-promoted catalyst activity was high, and it performed nearly identically to the ICI74-1 industrial system with a high cobalt content. Therefore, the economic viability of replacing cobalt with cheap rare-earth gangue was indicated as the cost of fused iron catalysts could significantly decrease. Its use in the iron system could decrease the cobalt content or even eliminate it, which was regarded as an unsubstitutable promoter for high-performance ammonia catalysts.

The scope of the available literature shows that although lanthanide oxides are not commonly used as an iron catalyst dopant, they undeniably benefit its various properties, including activity.

#### 4. Ruthenium-Based Catalysts

Although ruthenium is considered one of the most active phases in the ammonia synthesis reaction among the transition metal family, the element in its metallic form, without proper structuring, does not display any significant catalytic performance [58,59]. An efficient catalyst is obtained only via the strong dispersion of ruthenium into nanometric crystallites with a predominant share of defective surface structures of high surface energy and further enhancement in their electron donor capabilities. It is achieved through the use of properly selected supports or promoters. Lanthanide oxides have often been used in recent years due to their unique and desirable properties.

In ruthenium systems, alkali metal ions, alkaline earth, and rare-earth ions are usually used as promoters. A broad characterisation of these ions' influence on ruthenium catalytic activity was undertaken by Aika et al. [60], who studied Ru/MgO systems. The activities of the studied catalysts are summarised in Table 3.

**Table 3.** Promoter (M) effect on 2 wt.% Ru/MgO (M/Ru = 1 mol ratio) for NH<sub>3</sub> synthesis under 80 kPa of N<sub>2</sub> + 3H<sub>2</sub>, at 588 K. Reproduced with permission from ref. [60]. © Elsevier 1992.

Promoter	Rate [ $\mu\text{mol}_{\text{NH}_3} \text{g}^{-1} \text{h}^{-1}$ ]
-	60
Na <sup>+</sup>	361
K <sup>+</sup>	536
Rb <sup>+</sup>	581
Cs <sup>+</sup>	690
Ca <sup>2+</sup>	135
Sr <sup>2+</sup>	113
Ba <sup>2+</sup>	213
La <sup>3+</sup>	115
Ce <sup>3+</sup>	100
Pr <sup>3+</sup>	129
Nd <sup>3+</sup>	140
Sm <sup>3+</sup>	86
Gd <sup>3+</sup>	93
Dy <sup>3+</sup>	118

A comparison of the activity of the promoted and non-promoted systems highlights the dire need to add promoters for effective catalyst performance. Alkali metal cations (Cs<sup>+</sup>, Rb<sup>+</sup>, K<sup>+</sup>, and Na<sup>+</sup>) induced the strongest effect; however, the influence of alkaline earth cations (especially Ba<sup>2+</sup>) and lanthanides was also noticeable, albeit to a lesser extent. The promoting effect of these metals is well established, and numerous studies indicate caesium, potassium, and barium as those with a dominant promoting power. Compounds containing selected cations are primarily assigned an electronic function, facilitating the dissociation of adsorbed nitrogen molecules and supporting the product's desorption by directly donating electrons from the active metal surface to the lowest unoccupied molecular orbital (LUMO) of dinitrogen or mediating their transport. However, there is no shortage of studies attributing other functions to these compounds. However, alkali promoters tend to increase the susceptibility of an active phase to hydrogen poisoning as they facilitate hydrogen adsorption to the degree that it starts competing with nitrogen adsorption. Such an effect was not observed by Kadowaki et al. [61] in the lanthanide oxide-promoted Ru catalysts, where in the case of the Ru-Sm<sub>2</sub>O<sub>3</sub>/Al<sub>2</sub>O<sub>3</sub> system, the activity increase caused by a decrease in the activation energy was free of the hydrogen retardation effect.

Aika et al. [60] suggested the electronic promotion function of lanthanide cations. They demonstrated nearly double the activity of Ln-promoted catalysts relative to the activity of the non-promoted Ru/C system. Ni et al. [62] studied ruthenium catalysts deposited on activated carbon and promoted with La, Ba, or K. The results of this research indicated

that the addition of La contributes to the increase in the amount of adsorbed  $N_2$  on the surface of the active phase, a decrease in the amount of  $H_2$ , as well as an increase in the dispersion of Ru and an improvement in the carbon support stability. Murata et al. [63,64] demonstrated that La, Ce, and Sm nitrates(V) are more efficient electron promoters of the Ru/ $Al_2O_3$  system than  $CsNO_3$ . The lanthanide nitrates contributed to a similar catalyst activity with a 2.5 times smaller amount of promoter added. Niwa et al. [65] proved that lanthanide oxides as supports are a far more efficient form of these metals than their cations (Figure 2).

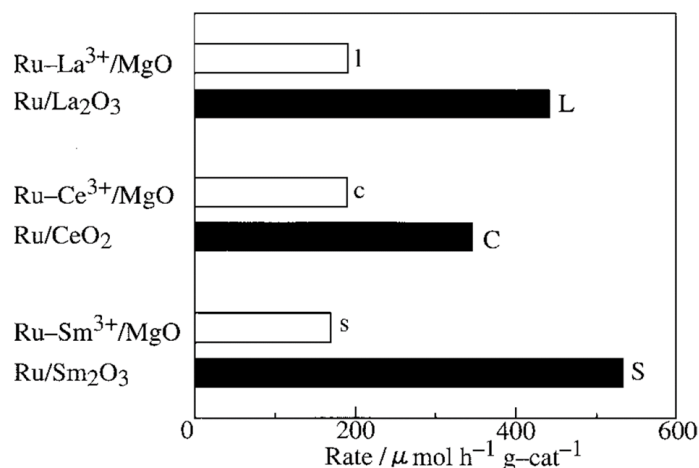


**Figure 2.** Ammonia synthesis rate at 588 K on 1 g of supported catalyst with 1.0 wt.% of Ru; 0.1 MPa,  $H_2/N_2 = 3$ . Comparison of lanthanide promoter and support. All the samples were reduced at 773 K. Ru/lanthana (promoter) = 1/1 (mol/mol). Reproduced with permission from ref. [65]. © Elsevier 1996.

As Niwa et al. [65] illustrated, ruthenium catalysts deposited on lanthanide oxides were nearly twice as active as Ru/MgO reference systems promoted by the corresponding lanthanide cation. The increased activity was attributed to strong metal–support interactions (SMSIs), which resulted in defective  $Ln_2O_{3-x}$  support species formed under reducing conditions, containing stable oxygen vacancies in their lattice abundant with electrons. The vacancies near ruthenium particles are a source and a channel for electrons transferred to the metal surface [65,66], leading to a localised increase in electron density. The author suggested that the difference in activity may also be caused by the limited stability of promoters in the form of salts under the  $NH_3$  synthesis reaction conditions [3,60], their degradation, and the loss of beneficial properties [67].

Sato et al. [68] investigated the activity of Ru/ $Pr_2O_3$  catalysts (Figure 3). For this system, he recorded nearly twice the reaction rate at 1 MPa, compared to other Ru/support catalysts regarded in the literature as those of the highest activity: Ba-Ru/AC and Cs-Ru/MgO [8]. Due to the remarkable performance, the system composition and synthesis method were patented [69]. As the reason for the extraordinary activity, the authors pointed to the morphology of the catalyst surface: ruthenium was present as a nanolayer covering the entire surface of the support (Figure 4). As argued by the authors, the nanolayer was formed due to a redox reaction between the  $Ru_3(CO)_{12}$  precursor and the  $Pr_6O_{11}$  phase at the catalyst synthesis stage, which prevented the aggregation of ruthenium crystallites. The area was created with many faults and terraces structurally similar to the active B5 sites, uncoordinated sites with optimal  $N_2$  adsorption energy [70]. Additionally, due to the high basicity of the support, it was possible to efficiently transfer the charge to the metal surface and facilitate the dissociation of adsorbing  $N_2$  molecules.

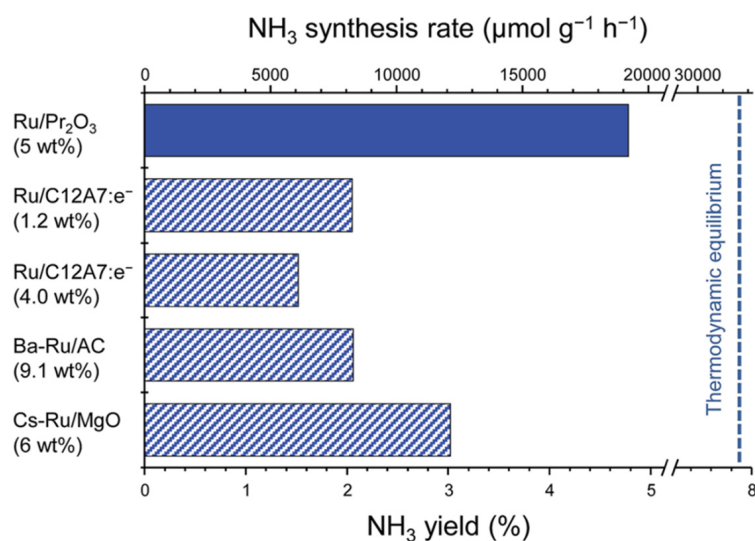


**Figure 3.** Catalytic performance of supported Ru catalysts for NH<sub>3</sub> synthesis at 1 MPa. Reaction conditions: catalyst, 0.2 g; reactant gas, H<sub>2</sub>/N<sub>2</sub> = 3 with a flow rate of 60 cm<sup>3</sup> min<sup>-1</sup>; reaction temperature, 400 °C. Reproduced with permission for ref. [68]. © The Royal Society of Chemistry 2017.

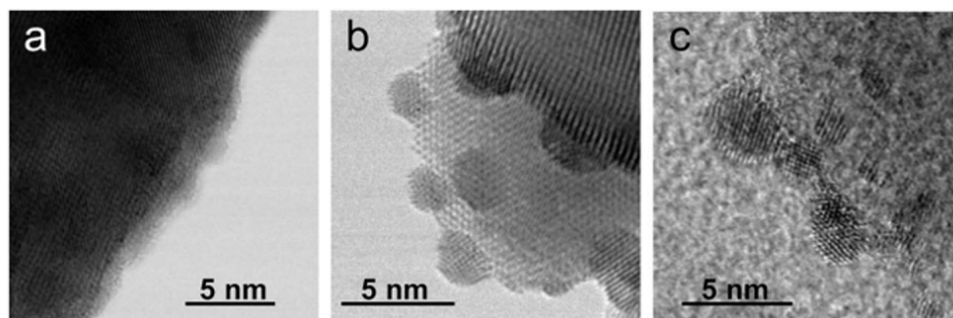


**Figure 4.** HR-STEM images of (a) Ru/Pr<sub>2</sub>O<sub>3</sub>, (b) Ru/CeO<sub>2</sub>, and (c) Ru/MgO after H<sub>2</sub> reduction. Reproduced with permission for ref. [68]. © The Royal Society of Chemistry 2017.

Further studies of the Ru/Pr<sub>2</sub>O<sub>3</sub> system were also undertaken by Imamura et al. [71], who focused on analysing the NH<sub>3</sub> synthesis reaction kinetics carried out with this catalyst. The results of his experiments indicated that ruthenium catalysts deposited on lanthanide oxides are characterised by a much lower susceptibility to hydrogen and product poisoning, in contrast to many other ruthenium systems burdened with this flaw [72–74]. The authors attributed the differences in properties to the basicity of lanthanide oxides and their greater stability under reaction conditions compared to electron promoters such as Cs<sub>2</sub>O, whose action is strongly inhibited by adsorbing hydrogen [75].

Miyahara et al. [76], encouraged by the high activity of ruthenium catalysts deposited on praseodymium oxide, tested most of the lanthanide oxides as supports and compared their activity with the Ru/MgO contact (Figure 5). They demonstrated the differentiated activity of catalytic systems depending on the support used. Systems deposited on lighter oxides were characterised by higher activity than the reference system (Ru/MgO) (in descending order: Pr<sub>2</sub>O<sub>3</sub> > CeO<sub>2</sub> > La<sub>2</sub>O<sub>3</sub> > Nd<sub>2</sub>O<sub>3</sub> > Sm<sub>2</sub>O<sub>3</sub> > Gd<sub>2</sub>O<sub>3</sub>). Catalysts deposited on heavier oxides: Tb<sub>2</sub>O<sub>3</sub>, Ho<sub>2</sub>O<sub>3</sub>, Er<sub>2</sub>O<sub>3</sub>, and Yb<sub>2</sub>O<sub>3</sub> displayed lower activity, which was caused by the low specific surface area of the supports conducive to the aggregation of metal crystallites and the consequent decrease in the number of active sites at the surface.

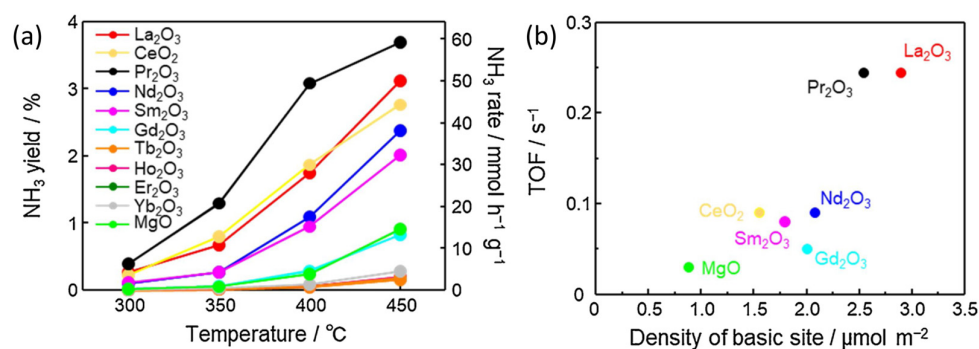


**Figure 5.** (a) Effect of temperature on ammonia synthesis activity of Ru/lanthanoid oxide catalysts at 1.0 MPa; (b) turnover frequency (TOF) of ammonia synthesis at 400 °C as a function of the density of basic sites in Ru/lanthanoid oxide catalysts. Reproduced with permission for ref. [76]. © Elsevier 2021.

The kinetic analysis carried out by Miyahara et al. [76] indicated that compared to Ru/MgO, all systems deposited on lanthanide oxides are characterised by high resistance to hydrogen poisoning (order of reaction to H<sub>2</sub> ~ 0), which is due to the presence of electrons in the f orbitals of lanthanides. Miyahara also drew attention to the negative, low value of the exponent describing the reaction order to NH<sub>3</sub>, which suggests that the activity of these catalysts may be limited by the opposite reaction: the decomposition of ammonia, occurring under conditions of an increased concentration of the product in the gas. The author also presented a correlation between the catalyst's surface activity (TOF) and the density of basic sites on its surface (Figure 5b); the most active catalysts also exhibited the highest number of basic sites.

Among lanthanide oxides, cerium oxide attracts significant attention from researchers. In all reports, the high activity of such systems, good dispersion of deposited ruthenium, and the support's participation in increasing the electron density on the active phase crystallites are indicated. The studies point to several factors that are responsible for such a state. Luo et al. [77] and Li et al. [78] reported the occurrence of SMSI interactions, increasing the electron density of the catalyst surface. Ma et al. [79] and Liu et al. [80] demonstrated the participation of oxygen vacancies (formed on the reduced surface of the support) in the charge transport, support of nitrogen dissociation, and inhibition of hydrogen poisoning. The works of Lin et al. [81,82], Wang et al. [83,84], and Li et al. [85] indicated the relationship between the structure of the ceria resulting from the method of its synthesis and the occurrence of defects in the lattice, i.e., the number of oxygen vacancies modifying the electron donor capacity. The broad studies of Ru/CeO<sub>2</sub> conducted by researchers from Fuzhou University resulted in several patents concerning its composition and preparation [86,87]. As reported by Manaka et al. [88], the sorption properties of the Ru/CeO<sub>2</sub> system, the strength of the Ru-CeO<sub>2</sub> interactions, and, consequently, the activity are also influenced by the method of synthesis of the catalyst itself, and more precisely by the type of Ru precursor used. Luo et al. [77], Han et al. [89], Ogura et al. [90,91], and Zhang et al. [92] also suggested the possibility of controlling the deflection of the cerium oxide to modify the catalyst properties and increasing the electron density on Ru via the introduction of other lanthanide cations (La, Pr, and Sm) into the crystal lattice. Similarly, Ma et al. [93] and Wu et al. [94,95] reported that it can also be performed by incorporating transition metals such as Zr and Ti. Ma et al. [79] and Liu et al. [80] indicated the possibility of a further activation of catalysts deposited on ceria and other lanthanide oxides by introducing Cs<sup>+</sup>, K<sup>+</sup>, and Ba<sup>2+</sup> ions, which reduced the work function of electrons from the active phase surface.

Another widely studied ruthenium catalyst support type is MgO-Ln<sub>2</sub>O<sub>3</sub> mixed oxides [96–99]. The research groups of Saito et al. and Javaid et al. independently observed a synergy effect resulting from such a fusion. The catalyst deposited on the mixed oxide was significantly more active than the Ru/MgO system. In addition, using such a mixture

of oxides is economically justified as it reduces the cost of the supports due to the relative inexpensiveness of MgO compared to lanthanide oxides. The first report on using this support type can be found in the works of Saito et al. [96]. They demonstrated the superiority of mixed MgO-CeO<sub>2</sub> oxides over MgO and CeO<sub>2</sub> as supports of ruthenium catalysts (Figure 6).

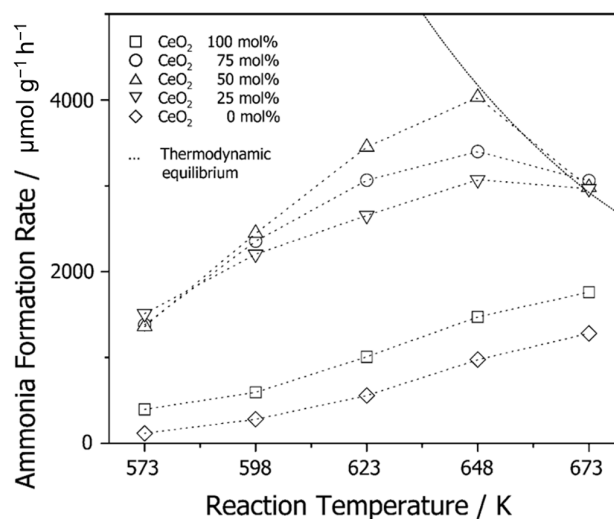


**Figure 6.** Temperature dependencies of ammonia formation rates on Ru/(MgO–CeO<sub>2</sub>) catalysts with various contents of CeO<sub>2</sub>. Reproduced with permission from ref. [96]. © Springer Nature 2006.

The Ru/MgO–CeO<sub>2</sub> catalysts displayed higher activity in the tested temperature range than the Ru/MgO and Ru/CeO<sub>2</sub> systems. Two factors were assumed to cause such a state. It was shown that using mixed oxides increased the interaction strength between Ru and the support, accelerating the partial reduction of cerium oxide. Partially reduced ceria, CeO<sub>2-δ</sub>, constituted the electron source, causing a local increase in electron density at the ruthenium (Ru<sub>δ-</sub>) atoms. This was attributed to the weakening of the dinitrogen bond and allowed for its facilitated chemisorptive dissociation. The second factor responsible was the higher dispersion of Ru on the surface of the mixed oxides compared to single ones. It increased the contact area between the active phase and the support, resulting in a more efficient electron transfer between the two phases.

Studies on ruthenium catalysts deposited on mixed magnesium–lanthanide oxides have been conducted by Javaid et al. [97–99]. Work [97] described using MgO–Tb<sub>2</sub>O<sub>3</sub>, MgO–Dy<sub>2</sub>O<sub>3</sub>, MgO–Ho<sub>2</sub>O<sub>3</sub>, MgO–Er<sub>2</sub>O<sub>3</sub>, and MgO–Yb<sub>2</sub>O<sub>3</sub> as the ruthenium supports. Among the catalysts produced, the Ru/MgO–Er<sub>2</sub>O<sub>3</sub> system was the most active in ammonia synthesis. Also, the effect of the Mg/Er molar ratio on the specific surface area and activity of Ru/MgO–Er<sub>2</sub>O<sub>3</sub> catalysts was determined (Figure 7).

The molar ratio of Mg/Er affects the size of the specific surface area and the activity of catalysts. However, researchers did not achieve the beneficial effect of oxide combination that Saito et al. did [96]. It was found that the optimal molar ratio of Mg/Er is equal to 25, as it provides a satisfactory development of the specific surface area and activity greater than Ru/MgO yet comparable to Ru/Er<sub>2</sub>O<sub>3</sub>. The observed increase in the activity of the Ru/MgO–Er<sub>2</sub>O<sub>3</sub> catalyst (at a molar ratio of Mg/Er = 25) was explained by the phenomenon of the preferential deposition of ruthenium particles on the surface of Er<sub>2</sub>O<sub>3</sub>.

Despite their short history, ruthenium catalysts have already found their way into industrial practice and the consciousness of researchers. However, there is still much room for optimisation, and in the coming years, many reports about further discoveries are planned [7,8], mainly involving lanthanide oxides. Despite all its advantages, ruthenium remains a very expensive metal, which is why other metals, such as cobalt, gain many researchers' attention.

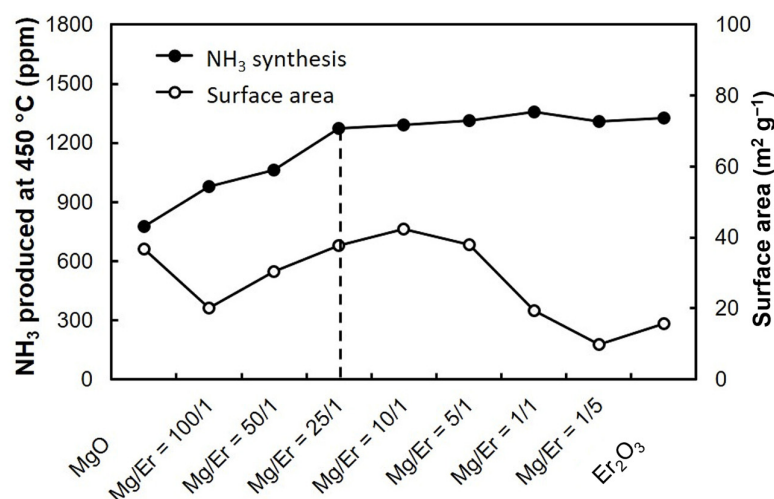


**Figure 7.** A comparison between the surface areas and the activity trends of Ru/MgO–Er<sub>2</sub>O<sub>3</sub> catalysts at 450 °C, 0.1 Mpa, and H<sub>2</sub>/N<sub>2</sub>. Reproduced with permission from ref. [97]. © Elsevier 2020.

### 5. Cobalt-Based Catalysts

Despite the great potential, cobalt metal displays only marginal catalytic activity in its unmodified and raw form [100,101], like iron and ruthenium. The use of cobalt as an independent active phase is a relatively recent issue. Originally, cobalt was used as a structural promoter of an iron catalyst, e.g., as reported by Smith et al. [102,103] and Kaleńczuk et al. [104,105]. Its operation consisted of modifying the catalyst reduction, as a result of which a more developed interfacial contact surface was created. In addition, cobalt stabilised the surface of the iron under reaction conditions, preventing it from sintering. These factors led to an increase in the activity of the catalyst.

The first reports of developing an active cobalt-based supported catalyst can be attributed to Hagen et al. [106], who described a barium-promoted cobalt system deposited on activated carbon. This contact showed nearly 40% higher activity than the commercial iron catalyst KMI and a lower susceptibility to product poisoning.

Similar observations are presented by Hagen et al. in a study [107], which focused on barium-promoted bimetallic Co-Fe catalysts. The results confirmed the low activity of unpromoted cobalt (even though it was dispersed on a carbon support). They indicated the need to modify its surface's adsorption and dissociative capacity to obtain a high-activity catalyst. The author also demonstrated that alkaline earth metals have a stronger promoting effect than alkali metals, with the greatest increase in activity obtained by adding barium (more than two orders of magnitude compared to the non-promoted catalyst; a 281-fold activity increase) [107]. Hagen also pointed out that the cobalt systems promoted with barium exhibited resistance to NH<sub>3</sub> poisoning, similarly to the ruthenium catalysts, but in contrast, showed very low susceptibility to hydrogen inhibition.

Hagen's work emphasised the potential hidden in cobalt catalysts, whose operation was then poorly understood. It encouraged their optimisation in terms of composition or synthesis methods, among others. Research on cobalt catalysts deposited on graphitised activated carbon was also carried out by Raróg-Pilecka et al. [108] and Tarka et al. [109]. The analyses concerned the influence of catalyst preparation routes on its properties. It has been demonstrated that the smallest particle sizes and high activity are achieved via the deposition of small amounts of the active phase precursor on a high-surface-area support, calcination, and subsequent introduction of the promoter into the catalytic system. The catalyst obtained this way was much more active than the commercial KMI iron system, especially at high levels (above 11%<sub>mol.</sub>) of ammonia content in the gas. Still, it displayed almost twice the activation energy. Despite using a high-surface-area support, the metal dispersion obtained was relatively low, as Karolewska et al. pointed out [110], indicating the possibility of using cerium as a structural promoter of cobalt in Ba-Co/C systems.

However, an increase in dispersion and a decrease in the average size of cobalt particles (and a consequent increase in catalyst activity) occurred only when the cobalt and cerium promoter precursors were introduced simultaneously. The action of ceria promoter in supported systems manifests itself mainly at the stage of contact synthesis. The presence of a cerium and cobalt mixture induces a better dispersion and segregation of  $\text{Co}_3\text{O}_4$  phase particles formed via calcination, which, due to the reduction, transforms into a metallic phase strongly dispersed on the support. In work [109], Tarka et al., on the other hand, showed that adding barium counteracts the carbon support's methanation, reducing the sintering of active phase particles under reaction conditions. In addition, even a small promoter content, which tends to localise on cobalt particles, yields a significant effect.

The change in the cobalt catalyst development direction was initiated by the work of Raróg-Pilecka et al. [111]. The authors used activated carbon not as a catalyst support but as a matrix to create high-surface-area support-free catalysts via the templating method [112,113]. Depositing a cobalt precursor or a mixture of cobalt and cerium precursors on a carbon matrix, subsequently calcining the material, and then burning the matrix led to the creation of a material with an extensive and developed porous structure, which was a reproduction of the carbon template. Oxide materials were impregnated with barium nitrate. In the studies, cerium was primarily assigned a structural function; it developed the surface area of cobalt in the Co+Ce system, but no activating effect was observed. Due to the higher reaction rate obtained with the Co+Ba catalyst, an order of magnitude higher than the Co+Ce system, barium was assigned a cobalt-activating effect. The highest reaction rate (25 times higher than the Co+Ce catalyst) was obtained for the co-promoted Co+Ce+Ba system. This is due to the synergistic action of both additives: the development of the cobalt surface by cerium and its activation by barium. The synergistic interaction was also observed in support-free cobalt catalysts obtained via the co-precipitation method, investigated by Raróg-Pilecka et al. [114]. The co-precipitation synthesis method of a cobalt-based catalyst and its optimal conditions were patented and often applied in subsequent works of this research group [115].

The results of the measurements carried out by Raróg-Pilecka et al. indicated the synergy effect occurring due to the co-promotion of cobalt with cerium–barium compounds. It was manifested by a significant increase in the surface activity (TOF) of the co-promoted catalyst compared to single-promoted systems. The TOF of the Co/Ce/Ba catalyst increases by more than twice as much in relation to the Co/Ba system and by an order of magnitude in relation to the Co/Ce catalyst, i.e., in a similar manner to systems obtained via the carbon matrix templating method [111]. The authors of [114] also pointed to the extended functionality of barium in the system; in addition to its electronic action, it was also supposed to exhibit some features of a structural promoter, namely to prevent the sintering of active phase particles under reaction conditions.

Lin et al. presented their observations on the operation of barium in Ba/Co/Ce systems in the paper [116]. According to the author, adding barium modified the cobalt surface and increased the amount of  $\text{H}_2$  and  $\text{N}_2$  adsorbing on the catalyst surface. Lin also stated that an excess of barium had an adverse effect; it led to a decrease in the number of  $\text{H}_2$  adsorption sites and reduced the surface activity. The presence of a certain optimum for the barium promoter amount, which leads to the highest activity of the cobalt catalyst, was also indicated by Tarka [109]. According to Zybert et al. [117], the negative effect of barium excess is caused by the surface enrichment phenomenon [118]. A migration of barium compounds (under reaction conditions) to the surface of cobalt particles occurs due to the system's tendency to reduce the surface's free energy, decreasing the interfacial surface between the active phase and reactants.

It is worth noting that the observed synergy effect in the case of the Co/Ce/Ba systems [114,119,120] results in higher activity than would result from the summation of the activities of the single-promoted system. As Tarka et al. argued [121], the reason for the observed added value was the in situ formation of small amounts of a barium cerate phase ( $\text{BaCeO}_3$ ) at the catalyst activation stage through the reaction of the Ba and

Ce promoter precursors. This compound is characterised by significant basicity [122], increases the electron density on the surface of the active phase, reduces the impact of hydrogen poisoning [123], and contributes to the stabilisation of highly active [124,125] cobalt in HCP phases under reaction conditions. In her other work concerning barium and ceria-promoted cobalt catalyst, Tarka et al. [126] indicate that exceeding the 1:1 molar ratio of Ba to Ce may hinder the structural action of ceria. Then, decrease in the catalyst activity is observed, caused by surface area shrinkage and the accumulation of barium on the Co particles, leading to active site blocking.

In a study by Karolewska et al. [119] on the influence of cerium content on the properties of co-promoted cobalt systems, it was demonstrated that in addition to its structural, i.e., surface-developing effect, cerium oxide also prevents the sintering of cobalt particles at the calcination stage and during the  $\text{NH}_3$  synthesis reaction. In a study [119], ceria was also proven to stabilise the cobalt in the HCP phase under reaction conditions by increasing the phase transition temperature to its FCC form. To some extent, cerium also hindered the reduction of the  $\text{Co}_3\text{O}_4$ , that is, increased the reaction temperature.

In a study by Patkowski et al. [127] concerning the influence of the precursor calcination method on the properties of Co/Ce/Ba catalysts, the structural function of  $\text{CeO}_2$  as a promoter was also confirmed. The calcination process length and conditions were related to the resulting crystallinity of the promoters and the strength of their interactions. Elongated calcination induced a better crystallisation of  $\text{CeO}_2$  and  $\text{BaCeO}_3$  promoter phases, leading to significant activation of the cobalt surface and improved adsorption and dissociative capacity. However, the side effect was the intensification of sintering processes and a significant decrease in the specific surface area of the catalyst. The higher crystallinity of the promoters translated to an increased share of the HCP cobalt phase stabilised by them, thanks to which, the activity, especially the TOF, was high.

Cerium oxide can also modify the electronic properties of the cobalt surface. The co-precipitated Co/ $\text{CeO}_2$  catalyst was investigated by Lin et al. [128]. The authors prepared a series of ceria-supported catalysts, which they differentiated by applying different atmospheres of the calcination process: air and hydrogen. The catalyst calcined in hydrogen showed higher activity, which the authors attributed to the increased presence of hydroxyl groups on the surface of cerium oxide. The  $\text{OH}^-$  groups reacted with hydrogen under reaction conditions to form an  $\text{H}_2\text{O}$  molecule, which, after desorbing from the  $\text{CeO}_2$  surface, provided sites of suitable energy for  $\text{N}_2$  adsorption [129]. The additional sites accelerated the  $\text{NH}_3$  synthesis reaction rate by reducing competition for adsorption sites on the cobalt metal surface. The authors also pointed to the diversity of the obtained catalysts regarding the amount of oxygen vacancies in the cerium oxide structure. A catalyst annealed in a reducing atmosphere displayed more vacancies, which supported the dissociation processes on cobalt particles.

Issues related to the influence of the structure of cerium oxide and the resulting presence of oxygen vacancies and their impact on the activity of Co/ $\text{CeO}_2$  catalysts are discussed by Lin et al. in the paper [130]. Employing hydrothermal synthesis, the authors prepared cerium oxides of three different structures, with particles in the polyhedral, nanorod, and cubic forms. Then, via impregnation with cobalt salt and the subsequent reduction of these materials, catalysts with cobalt crystallites partially incorporated into the structure of cerium oxide were obtained. The diversified structure of the oxides significantly affected the reducibility of the materials and their deflection, i.e., the concentration of oxygen vacancies. The polyhedral structure of cerium oxide displayed the highest degree of reduction, i.e., the presence of  $\text{Ce}^{3+}$  ions and the highest number of oxygen vacancies, and the related cobalt active phase was characterised by the highest electron density on its surface, the lowest electron binding energy, and the highest activity [130].

Another proof of ceria being an appropriate support material for cobalt catalysts was presented by Wang et al. [131]. It is established that using Co/ $\text{CeO}_2$  in ammonia synthesis is somewhat problematic as the Co nanoparticles are thermodynamically unstable and prone to sintering under reaction conditions. Wang et al. presented a method of stabilising Co

nanoparticles at high temperatures due to SMSIs via the introduction of dopamine during the catalysts synthesis stage and further removing carbon layers via thermal treatment in  $N_2$ . It was demonstrated that the interactions between  $CeO_2$  and Co are dependent on the temperature of  $N_2$  treatment and carbon removal, with these yielding the most active catalysts that were 5 times more active than the unmodified Co/ $CeO_2$  system (an increase from  $3.81 \text{ mmol}_{NH_3} \text{ g}_{cat}^{-1} \text{ h}^{-1}$  to  $19.12 \text{ mmol}_{NH_3} \text{ g}_{cat}^{-1} \text{ h}^{-1}$ , at  $425 \text{ }^\circ\text{C}$  and 1 MPa). The details of the Co/ $CeO_2$  system pretreatment or synthesis method to maximise catalyst performance were also patented by Lin et al. [132,133].

Extensive research on lanthanum oxide as a promoter of a cobalt catalyst for ammonia synthesis was conducted by Zybert et al. [134,135]. In a study [134], the authors focused on obtaining co-precipitated cobalt catalysts promoted with lanthanum and barium. There, the functions of particular promoters in the system were identified. Lanthanum oxide is a structural promoter and does not activate the cobalt phase; its addition significantly developed the system's specific surface area and prevented cobalt particle sintering under reaction conditions. Despite this, the reaction rate involving the Co/La system was very low. Barium has a structural and modifying effect; it displayed action duality, similar to Co/Ce/Ba systems [114,121]. Its presence stabilised the active phase particles under the reaction conditions, and the activity of barium-promoted cobalt was more than an order of magnitude greater than that of cobalt promoted by lanthanum alone. In a co-promoted system, the synergy effect was observed. Active phase surface area and productivity increased nearly twofold compared to the Co/Ba system. The authors also drew attention to the fact that the presence of lanthanum hindered (i.e., raised the temperature) the reduction of cobalt oxide. At the same time, this effect can be counteracted by adding barium to the Co/La system.

Zybert et al. [135] also demonstrated the influence of  $La_2O_3$  content on the properties of co-precipitated Co/La/Ba catalyst. The data confirmed the structural action of the  $La_2O_3$  promoter. The authors proved that the surface activity (TOF) of La-promoted catalysts was similar to the Ba-promoted system, regardless of the La amount, and averaged ca.  $0.14 \text{ s}^{-1}$  at 6.3 MPa and  $400 \text{ }^\circ\text{C}$ . Also, an increase in the co-promoted catalysts' reaction rate was observed with the increase in the La content (and simultaneous decrease in the Co loading). The reaction rate gradually increased from  $1.3 \text{ g}_{NH_3} \text{ g}_{Co}^{-1} \text{ h}^{-1}$  for the Co(75.1)/La(1.8)/Ba system to  $4.2 \text{ g}_{NH_3} \text{ g}_{Co}^{-1} \text{ h}^{-1}$  for the Co(28,8)/La(55.7)/Ba catalyst, which was interpreted as proof for the structural action of  $La_2O_3$ , i.e., the development of cobalt's surface area and its prevention of particle sintering. Zybert et al. suggested that other activating promoters must be introduced for cobalt-lanthanide-based catalysts to operate effectively.

Broad research on cobalt catalysts deposited on mixed magnesium–lanthanide oxides was conducted by Ronduda et al. [136–144]. They demonstrated that using mixed supports results in very active catalysts, similar to ruthenium-based systems [96–99].

Ronduda et al. [136] proved (Figure 8b, red bars) that Co/MgO- $Ln_2O_3$  catalysts containing 10 wt.% of Co obtained via the wet impregnation of co-precipitated, mixed MgO- $Ln_2O_3$  ( $Ln = La, Nd, Eu$ ) are highly active. The Co/Mg-Nd system displayed a slightly higher reaction rate than the Co/Mg-La and Co/Mg-Eu catalysts. Its advantageous performance was ascribed to several factors. Firstly, the increased surface density of medium-strength basic sites enhanced the active phase's electron-donating ability. MgO- $Nd_2O_3$  support was characterised by more than 10% higher density of basic sites than other supports. Secondly, the deposition of cobalt did not change the nature of the basic sites on the support surface but resulted in their denser distribution. The Co/Mg-Nd system was also slightly less prone to hydrogen poisoning due to the smaller share of strong hydrogen binding sites on the catalyst surface than its counterparts.

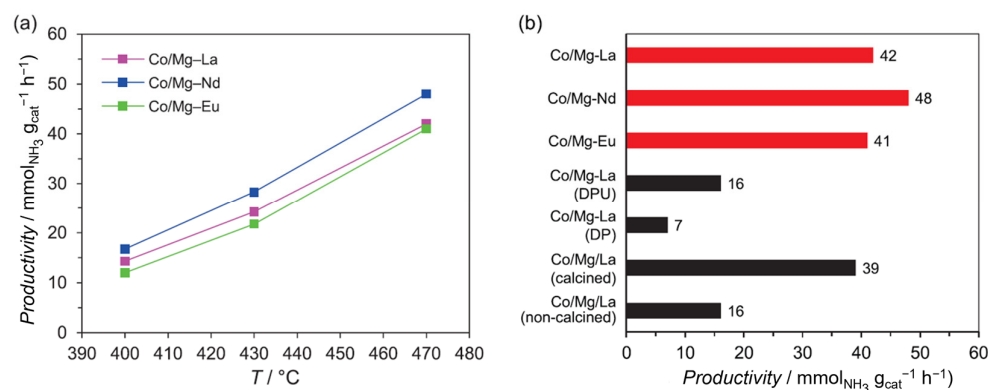


**Figure 8.** (a) Temperature dependence of the ammonia synthesis rates of Co/Mg-Ln catalysts. Reaction conditions: 6.3 MPa, H<sub>2</sub>/N<sub>2</sub> = 3,  $\dot{V} = 70 \text{ dm}^3 \text{ h}^{-1}$ . (b) NH<sub>3</sub> production rates of various catalysts. Reaction conditions: 6.3 MPa, H<sub>2</sub>/N<sub>2</sub> = 3,  $\dot{V} = 70 \text{ dm}^3 \text{ h}^{-1}$ , 470 °C. Except for Co/Mg-La, Co/Mg-Nd, and Co/Mg-Eu, the NH<sub>3</sub> production rates are taken from refs. [139,143]. Reproduced with permission from ref. [136]. © Elsevier 2022.

Ronduda et al. suggested the optimal Mg/Ln molar ratio in the mixed oxide supports. According to the researchers, an optimal Mg/Ln ratio promotes the formation of strong interactions between magnesium and lanthanide oxide, resulting in the partial incorporation of magnesium ions into the lanthanide oxide's structure. It reduces the oxygen-binding energy, promoting the formation of oxygen vacancies. The delocalisation of electrons, released by forming vacancies, induces a locally increased density, increasing the basic character of the mixed support surface. For the MgO-La<sub>2</sub>O<sub>3</sub> support, the optimal ratio was proposed as 7 [137], while for the MgO-Nd<sub>2</sub>O<sub>3</sub> support, it was proposed as 10 [138]. The systems deposited on optimised supports yielded the highest activities and displayed the highest surface areas and highest basicity, demonstrated by the highest densities of basic sites and highest share of ones of a strong nature. Relative to the activity exhibited by the Co/La<sub>2</sub>O<sub>3</sub> and Co/MgO catalysts, the Co/MgO-La<sub>2</sub>O<sub>3</sub> system with a Mg/La molar ratio equal to 7 exhibited a 2-fold and a 6.5-fold higher reaction rate, respectively. Analogously, the Co/MgO-Nd<sub>2</sub>O<sub>3</sub> system with an optimal Mg/Nd molar ratio of 10 yielded a reaction rate 1.5-fold higher than the Co/Nd<sub>2</sub>O<sub>3</sub> catalyst and as much as 13-fold higher than the Co/MgO catalyst.

The mixed-oxide-based catalyst synthesis method can also be optimised. Ronduda et al. demonstrated [139,143] that the selection of the metal precursor introduction method may alter the dispersion and size of the metal particles, as well as result in their different stability. A catalyst obtained via wet impregnation (WI) was characterised by a reaction rate more than three times higher compared to a catalyst obtained via the deposition–precipitation with urea method (DPU) and a reaction rate eight times higher compared to a catalyst obtained by the conventional deposition–precipitation method (DP). Productivity growth was also accompanied by a 4- to 8-fold increase in TOF [139]. Additionally, regardless of the Co precursor introduction method, the catalysts displayed similar thermal stability; however, the DP and DPU catalysts reduced at higher temperatures than the WI system.

Moreover, the surface of the WI catalyst was dominated by medium-strength basic sites, while sites of weak basicity dominated the surface of the DP and DPU catalysts. It was demonstrated that about 22% of hydrogen adsorption sites on the surface of the WI catalysts were located in the low-temperature region. In contrast, in the DPU catalyst, they accounted for only 6%, and almost no such sites were present in the DP system.

Ronduda et al. [142] also performed a kinetic characterisation of the most active catalyst and compared it to commercial iron-based systems (Figure 9).

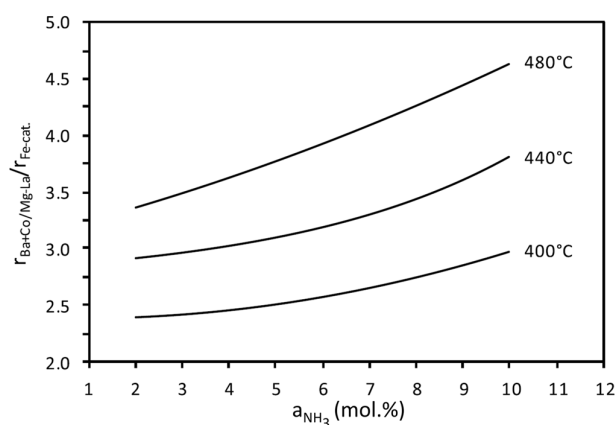


**Figure 9.** The ratio of  $\text{NH}_3$  synthesis reaction rates over the Ba+Co/Mg-La and the Fe-cat at various temperatures as a function of the average  $\text{NH}_3$  concentration in the gas phase ( $a_{\text{NH}_3}$ ). Activity measured at 9 MPa,  $\text{H}_2/\text{N}_2 = 3$ ,  $\dot{V} = 70 \text{ dm}^3 \text{ h}^{-1}$ . Reproduced with permission from ref. [142]. © Elsevier 2020.

The author demonstrated 2.5–4.5 times higher activity in the Ba+Co/Mg-La system compared to a commercial iron catalyst, depending on the reaction temperature and ammonia content in the reaction gas stream. The kinetic analysis of the catalysts indicated the cobalt-based system's higher resistance to product poisoning and its insensitivity to hydrogen poisoning, which distinguishes it from typical ruthenium-based catalysts. The results of Ronduda et al. confirmed that barium in Ba+Co/Mg-La systems contributes to an increase in the basicity of the active phase surface and modifies its adsorption capacity; i.e., Ba reduces the effect of hydrogen inhibition and reduces the adsorption energy of ammonia. It resulted in a 3.5-fold increase in activity relative to the unpromoted system and an increase in the system's thermostability [144]. In other studies [141], Ronduda et al. demonstrated that a Ba+Co/Mg-La system displayed an approximately two times higher reaction rate than the commonly used fused iron catalysts KM1 and P3-S-INS at 9 MPa and 400 °C.

It is also worth noting that in light of the present research, the activity of these catalysts is driven by two main factors: the basicity of the lanthanide support, as it determines the TOF of the active phase, and the active phase content, which determines the number of active sites as well as the cobalt particle size. In the study [140], concerning Co/MgO– $\text{La}_2\text{O}_3$  systems differing in cobalt loading, it was presented that regardless of the cobalt content, the TOF values for all systems were very similar ( $0.025 \text{ s}^{-1}$  at 6.3 MPa and 400 °C), which was achieved at an average cobalt particle size of ca. 20 nm. The recent studies by Zybert et al. [145] indicated an optimal size range of cobalt particles (20–30 nm), ensuring the highest activity of the given cobalt-based catalyst in the ammonia synthesis reaction. Increasing or decreasing the particle size, e.g., by altering the metal loading in the catalyst, will cause a decrease in activity. A drastic decrease in cobalt particle size below 0.5 nm may lead to total activity loss. Patkowski et al. also noted such a phenomenon in the studies of Co/ $\text{Nd}_2\text{O}_3$  systems with different cobalt loading amounts [146]. The TOF value averaged ca.  $0.125 \text{ s}^{-1}$  (6.3 MPa and 470 °C) for all systems with Co average particle sizes greater than 20 nm. Still, the TOF decreased visibly for the system with the lowest Co content (10 wt.%) and the smallest average Co particle size of 17 nm. The TOF decrease related to the change in the strength of hydrogen binding induced by the catalyst surface, as the high-energy to low-energy binding sites' number ratio grew exponentially with the decrease in the Co particle size. When the cobalt particle size decreased below 20 nm, the ratio exceeded 1.5, and the strong hydrogen binding sites dominated the catalyst surface. This is due to the multiplication of undercoordinated structures of cobalt, such as close-packed terraces, steps, and kinks at the cost of open surfaces [147], which bind  $\text{H}_2$  hydrogen stronger than flat surfaces [148,149]. This trade-off leads to the hydrogen poisoning of the catalysts, limiting their activity.

## 6. Conclusions and Perspectives

As emerges from the existing literature, among all the transition metals, the use of ruthenium or cobalt as an active phase for  $\text{NH}_3$  synthesis catalysts for the process conducted at mild conditions is explored the most often. These metals hold the most potential within the scope of decreasing the energy intensity of the synthesis process, despite their relatively high cost or limited availability, which is caused by their scarcity or high demand in competitive uses. Developing efficient catalysts suitable for industrial use remains a major challenge. Supports are often considered to lower the cost of the catalyst. They decrease the costly metal content, provide high metal dispersion, and allow the most efficient use of the metal particle surface. However, it is important to remember that contrary to popular belief, the high cost of catalysts is a manageable factor for their implementation [150–152]. As an average ammonia synthesis plant may require hundreds of tonnes of catalysts to operate, which may significantly increase capital expenditures, a 5- to 15-year period of efficient catalyst performance is often required and expected. Therefore, despite the major single investment cost of reactor filling and revamping, the share of the catalyst cost in the final product price is marginal as it is depreciated over the years of the plant's operation. It is estimated to correspond to ca. 0.5% of ammonia's total unit price, as the majority is constituted and driven by operational expenditures, electricity, and synthesis gas costs. Those may be decreased if the catalyst can operate at mild-temperature and -pressure conditions. This is why an industrially applicable catalyst that can provide an increase in ammonia yield of even a few per cent is economically justified, is in high demand, and can be considered despite its supposed high cost.

The available research indicates that lanthanides, as oxides or in another form, will drive the development of transition-metal-based catalysts for ammonia synthesis. They are especially valid within the scope of newly emerging uses of ammonia, i.e., utilising its molecules as hydrogen carriers and performing its synthesis through a process supplied with green hydrogen, generated through water electrolysis, and powered with renewable energy sources. Numerous reports indicate the suitability of lanthanide oxides as supports of ruthenium and cobalt catalysts. They are reliable and durable scaffolds for active phase deposition, with inherent flexibility due to a wide range of base cations and their characteristics, allowing for the tailoring of catalyst properties. This is often performed by altering the oxide synthesis and pretreatment methods and doping or mixing with other oxides, which allow for the modification and control of their morphology, particle dimensions, shapes, phase composition, and deflection of the lattices. These supports enable the active phase particles' size, dispersion, and electronic state regulation. They are also proven to stabilise them structurally under reaction conditions and prevent sintering or phase transitions. Lanthanide oxides can also provide a certain degree of electronic promotion: first, because they are inherently basic oxides; second, they can change their conductivity by generating defects, which aid in electron transfer. This enables increasing the charge density at the active phase surface, which is proven to be a key factor in elevating  $\text{NH}_3$  synthesis catalyst activity by facilitating dinitrogen adsorption and dissociation. They are also reported to display strong interactions with the active phase and, through their electronic influence, contribute to limiting the adsorption competition on the active sites, decreasing or even mitigating hydrogen and product poisoning.

Although lanthanide oxides constitute a potential platform for active catalysts for the  $\text{NH}_3$  synthesis process with low energy intensity, there are still some challenges on the path to industrial application, which further research needs to overcome. (1) Despite the electronic influence provided by lanthanide oxides, which favourably affects the catalyst's productivity, it alone is insufficient to yield a catalyst with suitable activity for industrial application. Still, as numerous papers have indicated, introducing additional electronic promoters, such as alkaline or alkaline earth metal ions, is mandatory and crucial to maximise the catalyst performance. A catalyst can outperform commercial iron systems only when such promoter and lanthanide oxide influences synergise. In this respect, it is crucial to understand lanthanide oxide influence and gain insight into the relationship

between oxide properties and catalyst activity. It is especially important to learn how to maximise their influence, as lanthanide oxides, despite being cheaper than Co or Ru, are still costly materials and usually constitute the majority of supported or non-supported systems. Therefore, conducting studies on the recycling or regeneration of spent catalysts or the recovery of lanthanide oxides and transition metals is also encouraged, as there is a shortage of these. (2) Within the scope of expected catalyst longevity, the stability of lanthanide oxides may constitute a challenge regarding catalyst integrity. Lanthanide oxides are susceptible to the H<sub>2</sub>O and CO<sub>2</sub> in the environment [40], as they easily form hydroxycarbonates in the presence of these [153,154]. The hydroxylation process rate and degree increase with the lanthanide cation radius increase, which causes the lightest of oxides (usually those of most beneficial influence as supports or promoters) to be most susceptible. The process may occur during catalyst synthesis, forming, storage, handling, or reduction in the reactor, wherever an H<sub>2</sub>O-rich environment may be present. During the hydroxylation and incorporation of OH<sup>-</sup> into the lattice, a quasi-layered structure is formed [155], which increases the material's volume. Such expansion may cause the catalyst grains or moulds to be exposed to mechanical stress, leading to the loss of their structural integrity. Such sensitivity also relates to the mixed supports due to the inclusion of MgO, which is also highly susceptible to water vapour. Therefore, special care must be taken to limit such exposure, and research must be undertaken to improve the catalyst water resistance. (3) In addition to the above, forming catalysts based on lanthanide oxides is often problematic. Efficient catalyst shapes are essential for the process design and maximising the catalyst performance, as the given form influences the occurrence of pressure gradients within the catalyst bed, heat and mass transport processes, or the efficiency of a converter. Powders of lanthanide oxides may require a design process with high-pressure pressing or extrusion, high-temperature heat treatment, and the addition of binders or lubricants to be formed into an efficient catalyst shape, all of which may drastically alter the catalyst's properties, severely poison it, or disable it completely. They are inferior to commonly used catalyst support materials, such as alumina, titania, or carbon. Unfortunately, most of the presented studies do not discuss the subject of catalyst formation and concern the material's as-obtained powder form. Therefore, more attention must be paid to this matter, indicating that more research is necessary. New forming or synthesis methods may need to be developed to shape catalysts containing lanthanide oxides properly. (4) The structural integrity issues of lanthanide oxide-containing catalyst forms are connected to dangers in their industrial operation. Due to the mentioned reasons behind mechanical stress, catalyst crumbling may occur, inevitably leading to the formation of catalyst dust. This is especially dangerous as lanthanide oxides display excellent abrasive properties, generating a risk of damage and premature wear in installation elements due to mechanical corrosion. This constitutes an additional crucial reason for extended catalyst stability research.

The journey towards more sustainable and efficient ammonia synthesis processes is undeniably paved with innovation. Lanthanide oxides have demonstrated their value as excellent catalyst modifiers of broad influence, regardless of being supports or promoters. Yet, there is still much to explore and accomplish. Future research efforts should be directed towards the precise tailoring of catalysts. Pursuing catalysts operating at lower pressures and temperatures is a path to reduced energy consumption. The challenge is to develop novel catalytic systems that render the Haber–Bosch process more sustainable and environmentally friendly. By fine-tuning the composition catalysts, it is conceivable that greater efficiency and sustainability in ammonia synthesis can be achieved than using the currently presented pioneering systems. To achieve this goal, the synergy of interdisciplinary efforts is pivotal. Collaborations between chemists, materials scientists, and engineers will drive innovation. These collective efforts will pave the way for developing next-generation catalysts that harness the full potential of lanthanide oxides. This comprehensive review of lanthanide oxides in ammonia synthesis catalysts signifies a culmination of current knowledge and a launchpad for future discoveries. Lanthanide oxides present an opportunity to make the ammonia synthesis process greener and more environmentally responsible.

**Author Contributions:** Conceptualisation, W.P., M.Z. and W.R.-P.; investigation, W.P. and H.R.; writing—original draft preparation, W.P.; writing—review and editing, W.P., M.Z. and W.R.-P.; visualisation, W.P.; supervision, W.P. and W.R.-P. All authors have read and agreed to the published version of the manuscript.

**Funding:** This research received no external funding.

**Data Availability Statement:** All data are available within the paper.

**Conflicts of Interest:** The authors declare no conflict of interest.

## References and Notes

1. Liu, H. *Ammonia Synthesis Catalysts*; World Scientific: Singapore, 2013.
2. Smith, C.; Hill, A.K.; Torrente-Murciano, L. Current and future role of Haber–Bosch ammonia in a carbon-free energy landscape. *Energy Environ. Sci.* **2020**, *13*, 331–344. [[CrossRef](#)]
3. Kubota, J.; Aika, K.I. Infrared studies of adsorbed dinitrogen on supported ruthenium catalysts for ammonia synthesis. Effects of the alumina and magnesia supports and the cesium compound promoter. *J. Phys. Chem.* **1994**, *98*, 11293–11300. [[CrossRef](#)]
4. Faria, J.A. Renaissance of ammonia synthesis for sustainable production of energy and fertilizers. *Curr. Opin. Green Sustain. Chem.* **2021**, *29*, 100466. [[CrossRef](#)]
5. Foster, S.L.; Bakovic, S.I.P.; Duda, R.D.; Maheshwari, S.; Milton, R.D.; Minter, S.D.; Janik, M.J.; Renner, J.N.; Greenlee, L.F. Catalysts for nitrogen reduction to ammonia. *Nat. Catal.* **2018**, *1*, 490–500. [[CrossRef](#)]
6. Cheng, J.; Hu, P.; Ellis, P.; French, S.; Kelly, G.; Lok, C.M. Brønsted-Evans-Polanyi relation of multistep reactions and volcano curve in heterogeneous catalysis. *J. Phys. Chem. C* **2008**, *112*, 1308–1311. [[CrossRef](#)]
7. Marakatti, V.S.; Gaigneaux, E.M. Recent Advances in Heterogeneous Catalysis for Ammonia Synthesis. *ChemCatChem* **2020**, *12*, 5838–5857. [[CrossRef](#)]
8. Humphreys, J.; Lan, R.; Tao, S. Development and Recent Progress on Ammonia Synthesis Catalysts for Haber-Bosch Process. *Adv. Energy Sustain. Res.* **2021**, *2*, 2000043. [[CrossRef](#)]
9. Humphreys, J.; Tao, S. Advancements in Green Ammonia Production and Utilisation Technologies. *Johns. Matthey Technol. Rev.* **2023**, *68*, 2000043. [[CrossRef](#)]
10. Feng, J.; Zhang, X.; Wang, J.; Ju, X.; Liu, L.; Chen, P. Applications of rare earth oxides in catalytic ammonia synthesis and decomposition. *Catal. Sci. Technol.* **2021**, *11*, 6330–6343. [[CrossRef](#)]
11. Gong, Y.; Li, H.; Li, C.; Bao, X.; Hosono, H.; Wang, J. Insight into rare-earth-incorporated catalysts: The chance for a more efficient ammonia synthesis. *J. Adv. Ceram.* **2022**, *11*, 1499–1529. [[CrossRef](#)]
12. Li, L.; Zhang, T.; Zhou, Y.; Wang, X.; Au, C.; Jiang, L. Review on catalytic roles of rare earth elements in ammonia synthesis: Development and perspective. *J. Rare Earths* **2022**, *40*, 1–10. [[CrossRef](#)]
13. Barbieri, M. Industrial Synthesis of Ammonia: A Patent Landscape. *SSRN J.* **2022**. [[CrossRef](#)]
14. Jordens, A.; Cheng, Y.P.; Waters, K.E. A review of the beneficiation of rare earth element bearing minerals. *Miner. Eng.* **2013**, *41*, 97–114. [[CrossRef](#)]
15. Gupta, C.K.; Krishnamurthy, N. Extractive metallurgy of rare earths. *Int. Mater. Rev.* **1992**, *37*, 197–248. [[CrossRef](#)]
16. Habashi, F. Extractive metallurgy of rare earths. *Can. Metall. Q.* **2013**, *52*, 224–233. [[CrossRef](#)]
17. Kilbourn, B.T. Lanthanide Oxides. In *Concise Encyclopedia of Advanced Ceramic Materials*; Brooks, R.J., Ed.; Pergamon Press: Oxford, UK, 1991; pp. 276–278. [[CrossRef](#)]
18. Eyring, L. The Binary Lanthanide Oxides: Synthesis and Identification. In *Synthesis of Lanthanide and Actinide Compounds*; Meyer, G., Morss, L.R., Eds.; Springer: Dordrecht, The Netherlands, 1991; pp. 187–224.
19. Huheey, J.E.; Keiter, E.A.; Keiter, R.L. *Inorganic Chemistry: Principles of Structure and Reactivity*; HarperCollins College Publishers: New York, NY, USA, 1993.
20. Seitz, M.; Oliver, A.G.; Raymond, K.N. The lanthanide contraction revisited. *J. Am. Chem. Soc.* **2007**, *129*, 11153–11160. [[CrossRef](#)] [[PubMed](#)]
21. Raymond, K.N.; Wellman, D.L.; Sgarlata, C.; Hill, A.P. Curvature of the lanthanide contraction: An explanation. *Comptes Rendus Chim.* **2010**, *13*, 849–852. [[CrossRef](#)]
22. Bernal, S.; Blanco, G.; Gatica, J.M.; Pérez-Omil, J.A.; Pintado, J.M.; Vidal, H. Chemical Reactivity of Binary Rare Earth Oxides. In *Binary Rare Earth Oxides*; Adachi, G., Imanaka, N., Kang, Z.C., Eds.; Springer: Dordrecht, The Netherlands, 2005; pp. 9–55.
23. Shannon, R.D. Revised effective ionic radii and systematic studies of interatomic distances in halides and chalcogenides. *Acta Crystallogr. Sect. A* **1976**, *32*, 751–767. [[CrossRef](#)]
24. Jia, Y.Q. Crystal radii and effective ionic radii of the rare earth ions. *J. Solid State Chem.* **1991**, *95*, 184–187. [[CrossRef](#)]
25. Schweda, E. Rare Earth Oxides. *Key Eng. Mater.* **1992**, *68*, 187–216. [[CrossRef](#)]
26. Haire, R.G.; Eyring, L. Chapter 125 Comparisons of the binary oxides. *Handb. Phys. Chem. Rare Earths* **1994**, *18*, 413–505. [[CrossRef](#)]
27. Borchert, Y.; Sonström, P.; Wilhelm, M.; Borchert, H.; Bäumer, M. Nanostructured praseodymium oxide: Preparation, structure, and catalytic properties. *J. Phys. Chem. C* **2008**, *112*, 3054–3063. [[CrossRef](#)]

28. Sonström, P.; Birkenstock, J.; Borchert, Y.; Schilinsky, L.; Behrend, P.; Gries, K.; Müller, K.; Rosenauer, A.; Bäumer, M. Nanostructured praseodymium oxide: Correlation between phase transitions and catalytic activity. *ChemCatChem* **2010**, *2*, 694–704. [[CrossRef](#)]
29. Antic-Fidancev, E.; Hölsä, J.; Lastusaari, M. Crystal field strength in C-type cubic rare earth oxides. *J. Alloys Compd.* **2002**, *341*, 82–86. [[CrossRef](#)]
30. Kang, Z.; Eyring, L. The Structural Basis of the Fluorite-Related Rare Earth Higher Oxides. *Aust. J. Chem.* **1996**, *49*, 981. [[CrossRef](#)]
31. Adachi, G.; Imanaka, N. The Binary Rare Earth Oxides. *Chem. Rev.* **1998**, *98*, 1479–1514. [[CrossRef](#)]
32. Rosynek, M.P. Catalytic Properties of Rare Earth Oxides. *Catal. Rev.-Sci. Eng.* **1977**, *16*, 111–154. [[CrossRef](#)]
33. Koehler, W.C.; Wollan, E.O. Neutron-diffraction study of the structure of the A-form of the rare earth sesquioxides. *Acta Crystallogr.* **1953**, *6*, 741–742. [[CrossRef](#)]
34. Douglass, R.M.; Staritzky, E. Crystallographic Data. 112. Samarium Sesquioxide, Sm<sub>2</sub>O<sub>3</sub>, Form B. *Anal. Chem.* **1956**, *28*, 552. [[CrossRef](#)]
35. Cromer, D.T. The Crystal Structure of Monoclinic Sm<sub>2</sub>O<sub>2</sub>. *J. Phys. Chem.* **1957**, *61*, 753–755. [[CrossRef](#)]
36. Pauling, L.; Shappell, M.D. The Crystal Structure of Bixbyite and the C-Modification of the Sesquioxides. *Zeitschrift für Krist.-Cryst. Mater.* **1930**, *75*, 128–142. [[CrossRef](#)]
37. Templeton, D.H.; Dauben, C.H. Lattice Parameters of Some Rare Earth Compounds and a Set of Crystal Radii. *J. Am. Chem. Soc.* **1954**, *76*, 5237–5239. [[CrossRef](#)]
38. Zhang, G.; Hattori, H.; Tanabe, K. Aldol Addition of Acetone, Catalyzed by Solid Base Catalysts: Magnesium Oxide, Calcium Oxide, Strontium Oxide, Barium Oxide, Lanthanum (III) Oxide and Zirconium Oxide. *Appl. Catal.* **1988**, *36*, 189–197. [[CrossRef](#)]
39. Busca, G. Acid and Basic Catalysts: Fundamentals. In *Heterogeneous Catalytic Materials*; Elsevier: Amsterdam, The Netherlands, 2014; pp. 57–101.
40. Sato, S.; Takahashi, R.; Kobune, M.; Gotoh, H. Basic properties of rare earth oxides. *Appl. Catal. A Gen.* **2009**, *356*, 57–63. [[CrossRef](#)]
41. Sato, S.; Takahashi, R.; Kobune, M.; Inoue, H.; Izawa, Y.; Ohno, H.; Takahashi, K. Dehydration of 1,4-butanediol over rare earth oxides. *Appl. Catal. A Gen.* **2009**, *356*, 64–71. [[CrossRef](#)]
42. Maitra, A.M. Determination of solid state basicity of rare earth oxides by thermal analysis of their carbonates. *J. Therm. Anal.* **1990**, *36*, 657–675. [[CrossRef](#)]
43. Rao, G.V.S.; Ramdas, S.; Mehrotra, P.N.; Rao, C.N.R. Electrical transport in rare-earth oxides. *J. Solid State Chem.* **1970**, *2*, 377–384. [[CrossRef](#)]
44. Imanaka, N. Physical and chemical properties of rare earth oxides. In *Binary Rare Earth Oxides*; Adachi, G., Imanaka, N., Kang, Z.C., Eds.; Springer: Dordrecht, The Netherlands, 2005; pp. 111–133.
45. Chandrashekar, G.V.; Mehrotra, P.N.; Rao, G.V.S.; Subbarao, E.C.; Rao, C.N.R. Semiconduction in non-stoichiometric rare earth oxides. *Trans. Faraday Soc.* **1967**, *63*, 1295. [[CrossRef](#)]
46. Aleksic, B.; Jovanovic, N.; Terlecki-Baricevic, A. In Proceedings of the Geterog. Katal. Tr. Mezhdunar. Simp. 3rd, 1978. p. 147.
47. Aleksic, B.; Bogdanov, S. Thermal analysis of the effect of samarium oxide on the reduction of precipitated ammonia synthesis catalyst. *Thermochim Acta* **1985**, *93*, 693. [[CrossRef](#)]
48. Mitov, I.; Klisurski, D.; Aleksic, B.; Gyurova, D.; Nikolov, G. Effect of samarium oxide (Sm<sub>2</sub>O<sub>3</sub>) on the reduction kinetics of precipitated iron catalysts for ammonia synthesis. Coprecipitated catalysts. *Izu Khim* **1984**, *17*, 305.
49. Berengarten, M.; Rudnitskii, L.; Zubova, I.; Alekseev, A.; Dmitrienko, L.; Mishchenko, S. Electron work function and specific catalytic activity of coprecipitated iron catalysts for ammonia synthesis promoted by rare earth element oxides. *Kinet. Katal.* **1974**, *15*, 250.
50. Dimitrov, M.; Rusev, R. *God. Viss. Khim.-Tekhnol. Inst. Sofia* **1980**, *26*, 103.
51. Rozin, A.; Komarov, V.; Efros, M.; Lemeshonok, G.; Eremenko, S. In Proceedings of the Vestsi Akad. Navuk BSSR Ser. Khim. Navuk, 1980. p. 35.
52. Rozin, A.; Komarov, V.; Efros, M. In Proceedings of the Vestsi Akad. Navuk BSSR Ser. Khim. Navuk, 1980. p. 27.
53. Dimitrov, M.; Rusev, R. *God. Viss. Khim.-Tekhnol. Inst. Sofia* **1980**, *26*, 111.
54. Dimitrov, M.; Rusev, R. *God. Viss. Khim.-Tekhnol. Inst. Sofia* **1980**, *26*, 126.
55. Karaslavova, K.; Anastasov, M.D. In Proceedings of Geterog. Katal. Tr. Mezhdunar. Simp. 3rd, 1978. p. 297.
56. Zakieva, K.; Rabina, P.; Zubova, I.; Khaustova, L.; Pavlova, N.; Kuznetsov, L. Effect of the oxides of rare (scandium, yttrium) and rare earth (lanthanum, praseodymium, erbium) elements on the kinetics of reduction of iron catalysts. *Tr. Mosk. Khim. Tekhnol. Inst.* **1973**, *73*, 120.
57. Yu, X.; Lin, B.; Lin, J.; Wang, R.; Wei, K. A novel fused iron catalyst for ammonia synthesis promoted with rare earth gangue. *J. Rare Earths* **2008**, *26*, 711–716. [[CrossRef](#)]
58. Aika, K.-I.; Hori, H.; Ozaki, A. Activation of nitrogen by alkali metal promoted transition metal I. Ammonia synthesis over ruthenium promoted by alkali metal. *J. Catal.* **1972**, *27*, 424–431. [[CrossRef](#)]
59. Rambeau, G.; Amariglio, H. Ammonia synthesis on ruthenium powder from 100 to 500 °C and hydrogenation of preadsorbed nitrogen down to –70 °C. *J. Catal.* **1981**, *72*, 1–11. [[CrossRef](#)]
60. Aika, K. Preparation and characterization of chlorine-free ruthenium catalysts and the promoter effect in ammonia synthesis 3. A magnesia-supported ruthenium catalyst. *J. Catal.* **1992**, *136*, 126–140. [[CrossRef](#)]
61. Kadowaki, Y.; Aika, K. Promoter Effect of Sm<sub>2</sub>O<sub>3</sub> on Ru/Al<sub>2</sub>O<sub>3</sub> in Ammonia Synthesis. *J. Catal.* **1996**, *161*, 178–185. [[CrossRef](#)]

62. Ni, J.; Lin, J.; Wang, X.; Lin, B.; Lin, J.; Jiang, L. Promoting Effects of Lanthan on Ru/AC for Ammonia Synthesis: Tuning Catalytic Efficiency and Stability Simultaneously. *ChemistrySelect* **2017**, *2*, 6040–6046. [[CrossRef](#)]
63. Murata, S. Preparation and characterization of chlorine-free ruthenium catalysts and the promoter effect in ammonia synthesis 2. A lanthanide oxide-promoted Ru/Al<sub>2</sub>O<sub>3</sub> catalyst. *J. Catal.* **1992**, *136*, 118–125. [[CrossRef](#)]
64. Murata, S.; Aika, K.; Onishi, T. Lanthanide Nitrates as Effective Promoters of a Ru/Al<sub>2</sub>O<sub>3</sub> Catalyst for Ammonia Synthesis. *Chem. Lett.* **1990**, *19*, 1067–1068. [[CrossRef](#)]
65. Niwa, Y.; Aika, K. The Effect of Lanthanide Oxides as a Support for Ruthenium Catalysts in Ammonia Synthesis. *J. Catal.* **1996**, *162*, 138–142. [[CrossRef](#)]
66. Niwa, Y.; Aika, K. Ruthenium Catalyst Supported on CeO<sub>2</sub> for Ammonia Synthesis. *Chem. Lett.* **1996**, *25*, 3–4. [[CrossRef](#)]
67. van Ommen, J.G.; Bolink, W.J.; Prasad, J.; Mars, P. The nature of the potassium compound acting as a promoter in iron-alumina catalysts for ammonia synthesis. *J. Catal.* **1975**, *38*, 120–127. [[CrossRef](#)]
68. Sato, K.; Imamura, K.; Kawano, Y.; Miyahara, S.; Yamamoto, T.; Matsumura, S.; Nagaoka, K. A low-crystalline ruthenium nano-layer supported on praseodymium oxide as an active catalyst for ammonia synthesis. *Chem. Sci.* **2017**, *8*, 674–679. [[CrossRef](#)] [[PubMed](#)]
69. Nagaoka, K.; Imamura, K.; Sato, K. Ammonia Synthesis Catalyst and Method for Producing Same. WO2016133213A1, 25 August 2016.
70. Song, Z.; Cai, T.; Hanson, J.C.; Rodriguez, J.A.; Hrbek, J. Structure and Reactivity of Ru Nanoparticles Supported on Modified Graphite Surfaces: A Study of the Model Catalysts for Ammonia Synthesis. *J. Am. Chem. Soc.* **2004**, *126*, 8576–8584. [[CrossRef](#)]
71. Imamura, K.; Miyahara, S.-I.; Kawano, Y.; Sato, K.; Nakasaka, Y.; Nagaoka, K. Kinetics of ammonia synthesis over Ru/Pr<sub>2</sub>O<sub>3</sub>. *J. Taiwan Inst. Chem. Eng.* **2019**, *105*, 50–56. [[CrossRef](#)]
72. Rosowski, F.; Hornung, A.; Hinrichsen, O.; Herein, D.; Muhler, M.; Ertl, G. Ruthenium catalysts for ammonia synthesis at high pressures: Preparation, characterization, and power-law kinetics. *Appl. Catal. A Gen.* **1997**, *151*, 443–460. [[CrossRef](#)]
73. Fernández, C.; Bion, N.; Gaigneaux, E.M.; Duprez, D.; Ruiz, P. Kinetics of hydrogen adsorption and mobility on Ru nanoparticles supported on alumina: Effects on the catalytic mechanism of ammonia synthesis. *J. Catal.* **2016**, *344*, 16–28. [[CrossRef](#)]
74. Tripodi, A.; Compagnoni, M.; Bahadori, E.; Rossetti, I. Process simulation of ammonia synthesis over optimized Ru/C catalyst and multibed Fe + Ru configurations. *J. Ind. Eng. Chem.* **2018**, *66*, 176–186. [[CrossRef](#)]
75. Inoue, Y.; Kitano, M.; Kishida, K.; Abe, H.; Niwa, Y.; Sasase, M.; Fujita, Y.; Ishikawa, H.; Yokoyama, T.; Hara, M.; et al. Efficient and Stable Ammonia Synthesis by Self-Organized Flat Ru Nanoparticles on Calcium Amide. *ACS Catal.* **2016**, *6*, 7577–7584. [[CrossRef](#)]
76. Miyahara, S.-I.; Sato, K.; Kawano, Y.; Imamura, K.; Ogura, Y.; Tsujimaru, K.; Nagaoka, K. Ammonia synthesis over lanthanoid oxide-supported ruthenium catalysts. *Catal. Today* **2021**, *376*, 36–40. [[CrossRef](#)]
77. Luo, X.; Wang, R.; Ni, J.; Lin, B.; Xu, X.; Wei, K. Effect of La<sub>2</sub>O<sub>3</sub> on Ru/CeO<sub>2</sub>-La<sub>2</sub>O<sub>3</sub> catalyst for ammonia synthesis. *Catal. Letters* **2009**, *133*, 382–387. [[CrossRef](#)]
78. Li, C.; Shi, Y.; Zhang, Z.; Ni, J.; Wang, X.; Lin, B.; Jiang, L. Improving the ammonia synthesis activity of Ru/CeO<sub>2</sub> through enhancement of the metal-support interaction. *J. Energy Chem.* **2021**, *60*, 403–409. [[CrossRef](#)]
79. Ma, Z.; Zhao, S.; Pei, X.; Xiong, X.; Hu, B. New insights into the support morphology-dependent ammonia synthesis activity of Ru/CeO<sub>2</sub> catalysts. *Catal. Sci. Technol.* **2017**, *7*, 191–199. [[CrossRef](#)]
80. Liu, P.; Niu, R.; Li, W.; Wang, S.; Li, J. The effect of barium-promoted for microsphere Ru/CeO<sub>2</sub> catalysts in ammonia synthesis. *Energy Sources Part A Recovery Util. Environ. Eff.* **2018**, *41*, 689–699. [[CrossRef](#)]
81. Lin, J.; Zhang, L.; Wang, Z.; Ni, J.; Wang, R.; Wei, K. The effect of Ag as a promoter for Ru/CeO<sub>2</sub> catalysts in ammonia synthesis. *J. Mol. Catal. A Chem.* **2013**, *366*, 375–379. [[CrossRef](#)]
82. Lin, B.; Liu, Y.; Heng, L.; Wang, X.; Ni, J.; Lin, J.; Jiang, L. Morphology Effect of Ceria on the Catalytic Performances of Ru/CeO<sub>2</sub> Catalysts for Ammonia Synthesis. *Ind. Eng. Chem. Res.* **2018**, *57*, 9127–9135. [[CrossRef](#)]
83. Wang, X.; Ni, J.; Lin, B.; Wang, R.; Lin, J.; Wei, K. Highly efficient Ru/MgO–CeO<sub>2</sub> catalyst for ammonia synthesis. *Catal. Commun.* **2010**, *12*, 251–254. [[CrossRef](#)]
84. Wang, X.; Peng, X.; Zhang, Y.; Ni, J.; Au, C.T.; Jiang, L. Efficient ammonia synthesis over a core-shell Ru/CeO<sub>2</sub> catalyst with a tunable CeO<sub>2</sub> size: DFT calculations and XAS spectroscopy studies. *Inorg. Chem. Front.* **2019**, *6*, 396–406. [[CrossRef](#)]
85. Li, W.; Liu, P.; Niu, R.; Li, J.; Wang, S. Influence of CeO<sub>2</sub> supports prepared with different precipitants over Ru/CeO<sub>2</sub> catalysts for ammonia synthesis. *Solid State Sci.* **2020**, *99*, 105983. [[CrossRef](#)]
86. Lin, B.; Wu, Y.; Ni, J.; Lin, J.; Jiang, L. Ruthenium-Based Ammonia Synthesis Catalyst with Cerium Oxide as Carrier. CN110252295A, 20 September 2019.
87. Lin, B.; Wu, Y.; Ni, J.; Lin, J.; Jiang, L. Ruthenium-Based Ammonia Synthesis Catalyst Using Cerium Oxide as Carrier. CN109277100A, 29 January 2019.
88. Manaka, Y.; Nagata, Y.; Kobayashi, K.; Kobayashi, D.; Nanba, T. The effect of a ruthenium precursor on the low-temperature ammonia synthesis activity over Ru/CeO<sub>2</sub>. *Dalt. Trans.* **2020**, *49*, 17143–17146. [[CrossRef](#)] [[PubMed](#)]
89. Han, W.; Li, Z.; Liu, H. La<sub>2</sub>Ce<sub>2</sub>O<sub>7</sub> supported ruthenium as a robust catalyst for ammonia synthesis. *J. Rare Earths* **2019**, *37*, 492–499. [[CrossRef](#)]

90. Ogura, Y.; Sato, K.; Miyahara, S.I.; Kawano, Y.; Toriyama, T.; Yamamoto, T.; Matsumura, S.; Hosokawa, S.; Nagaoka, K. Efficient ammonia synthesis over a Ru/La<sub>0.5</sub>Ce<sub>0.5</sub>O<sub>1.75</sub> catalyst pre-reduced at high temperature. *Chem. Sci.* **2018**, *9*, 2230–2237. [[CrossRef](#)] [[PubMed](#)]
91. Ogura, Y.; Tsujimaru, K.; Sato, K.; Miyahara, S.I.; Toriyama, T.; Yamamoto, T.; Matsumura, S.; Nagaoka, K. Ru/La<sub>0.5</sub>Pr<sub>0.5</sub>O<sub>1.75</sub> Catalyst for Low-Temperature Ammonia Synthesis. *ACS Sustain. Chem. Eng.* **2018**, *6*, 17258–17266. [[CrossRef](#)]
92. Zhang, L.; Lin, J.; Ni, J.; Wang, R.; Wei, K. Highly efficient Ru/Sm<sub>2</sub>O<sub>3</sub>-CeO<sub>2</sub> catalyst for ammonia synthesis. *Catal. Commun.* **2011**, *15*, 23–26. [[CrossRef](#)]
93. Ma, Z.; Xiong, X.; Song, C.; Hu, B.; Zhang, W. Electronic metal-support interactions enhance the ammonia synthesis activity over ruthenium supported on Zr-modified CeO<sub>2</sub> catalysts. *RSC Adv.* **2016**, *6*, 51106–51110. [[CrossRef](#)]
94. Wu, Y.; Li, C.; Fang, B.; Wang, X.; Ni, J.; Lin, B.; Lin, J.; Jiang, L. Enhanced ammonia synthesis performance of ceria-supported Ru catalysts via introduction of titanium. *Chem. Commun.* **2020**, *56*, 1141–1144. [[CrossRef](#)]
95. Lin, B.; Chi, Z.; Wu, Y.; Ni, J.; Lin, J.; Jiang, L. Ruthenium-Based Ammonia Synthesis Catalyst with Ce-Ti Composite Oxide as Carrier and Preparation Method Thereof. CN110368933A, 25 October 2019.
96. Saito, M.; Itoh, M.; Iwamoto, J.; Li, C.-Y.; Machida, K. Synergistic Effect of MgO and CeO<sub>2</sub> as a Support for Ruthenium Catalysts in Ammonia Synthesis. *Catal. Lett.* **2006**, *106*, 107–110. [[CrossRef](#)]
97. Javaid, R.; Aoki, Y.; Nanba, T. Highly efficient Ru/MgO-Er<sub>2</sub>O<sub>3</sub> catalysts for ammonia synthesis. *J. Phys. Chem. Solids* **2020**, *146*, 109570. [[CrossRef](#)]
98. Javaid, R.; Nanba, T. Effect of preparation method and reaction parameters on catalytic activity for ammonia synthesis. *Int. J. Hydrogen Energy* **2021**, *46*, 35209–35218. [[CrossRef](#)]
99. Javaid, R.; Nanba, T. Effect of texture and physical properties of catalysts on ammonia synthesis. *Catal. Today* **2022**, *397–399*, 592–597. [[CrossRef](#)]
100. Rambeau, G.; Jorti, A.; Amariglio, H. Catalytic activity of a cobalt powder in NH<sub>3</sub> synthesis in relation with the allotropic transformation of the metal. *J. Catal.* **1985**, *94*, 155–165. [[CrossRef](#)]
101. Larson, A.T.; Brooks, A.P. Ammonia Catalysts. *Ind. Eng. Chem.* **1926**, *18*, 1305–1307. [[CrossRef](#)]
102. Smith, P.J.; Taylor, D.W.; Dowden, D.A.; Kembell, C.; Taylor, D. Ammonia synthesis and related reactions over iron-cobalt and iron-nickel alloy catalysts. *Appl. Catal.* **1982**, *3*, 303–314. [[CrossRef](#)]
103. Taylor, D.W.; Smith, P.J.; Dowden, D.A.; Kembell, C.; Whan, D.A. Ammonia synthesis and related reactions over iron-cobalt and iron-nickel alloy catalysts. Part I. Catalysts reduced at 853 K. *Appl. Catal.* **1982**, *3*, 161–176. [[CrossRef](#)]
104. Kaleńczuk, R.J. Effect of cobalt on the morphology and activity of fused iron catalyst for ammonia synthesis. *Appl. Catal. A Gen.* **1994**, *112*, 149–160. [[CrossRef](#)]
105. Kaleńczuk, R.J. Cobalt promoted fused iron catalyst for ammonia synthesis. *Int. J. Inorg. Mater.* **2000**, *2*, 233–239. [[CrossRef](#)]
106. Hagen, S.; Barfod, R.; Fehrmann, R.; Jacobsen, C.J.H.H.; Teunissen, H.T.; Ståhl, K.; Chorkendorff, I. New efficient catalyst for ammonia synthesis: Barium-promoted cobalt on carbon. *Chem. Commun.* **2002**, *11*, 1206–1207. [[CrossRef](#)] [[PubMed](#)]
107. Hagen, S.; Barfod, R.; Fehrmann, R.; Jacobsen, C.J.H.; Teunissen, H.T.; Chorkendorff, I. Ammonia synthesis with barium-promoted iron-cobalt alloys supported on carbon. *J. Catal.* **2003**, *214*, 327–335. [[CrossRef](#)]
108. Raróg-Pilecka, W.; Miśkiewicz, E.; Kepiński, L.; Kaszkur, Z.; Kielar, K.; Kowalczyk, Z. Ammonia synthesis over barium-promoted cobalt catalysts supported on graphitised carbon. *J. Catal.* **2007**, *249*, 24–33. [[CrossRef](#)]
109. Tarka, A.; Zybert, M.; Truskiewicz, E.; Mierzwa, B.; Kepiński, L.; Moszyński, D.; Raróg-Pilecka, W. Effect of a Barium Promoter on the Stability and Activity of Carbon-Supported Cobalt Catalysts for Ammonia Synthesis. *ChemCatChem* **2015**, *7*, 2836–2839. [[CrossRef](#)]
110. Karolewska, M.; Truskiewicz, E.; Wściseł, M.; Mierzwa, B.; Kepiński, L.; Raróg-Pilecka, W. Ammonia synthesis over a Ba and Ce-promoted carbon-supported cobalt catalyst. Effect of the cerium addition and preparation procedure. *J. Catal.* **2013**, *303*, 130–134. [[CrossRef](#)]
111. Raróg-Pilecka, W.; Miśkiewicz, E.; Kowalczyk, Z. Activated carbon as a template for creating catalyst precursors. Unsupported cobalt catalyst for ammonia synthesis. *Catal. Commun.* **2008**, *9*, 870–873. [[CrossRef](#)]
112. Schwickardi, M.; Johann, T.; Schmidt, W.; Schüth, F. High-Surface-Area Oxides Obtained by an Activated Carbon Route. *Chem. Mater.* **2002**, *14*, 3913–3919. [[CrossRef](#)]
113. Schüth, F. Endo- and Exotemplating to Create High-Surface-Area Inorganic Materials. *Angew. Chemie Int. Ed.* **2003**, *42*, 3604–3622. [[CrossRef](#)]
114. Raróg-Pilecka, W.; Karolewska, M.; Truskiewicz, E.E.; Iwanek, E.; Mierzwa, B. Cobalt Catalyst Doped with Cerium and Barium Obtained by Co-Precipitation Method for Ammonia Synthesis Process. *Catal. Lett.* **2011**, *141*, 678–684. [[CrossRef](#)]
115. Kowalik, P.; Antoniak-Jurak, K.; Wiercioch, P.; Raróg-Pilecka, W.; Zybert, M.; Tarka, A. A Method for Obtaining Promoted Cobalt Catalysts for Ammonia Synthesis. EP3318326A1, 9 May 2018.
116. Lin, B.; Liu, Y.; Heng, L.; Ni, J.; Lin, J.; Jiang, L. Effect of barium and potassium promoter on Co/CeO<sub>2</sub> catalysts in ammonia synthesis. *J. Rare Earths* **2018**, *36*, 703–707. [[CrossRef](#)]
117. Zybert, M.; Wszyńska, M.; Tarka, A.; Patkowski, W.; Ronduda, H.; Mierzwa, B.; Kepiński, L.; Sarnecki, A.; Moszyński, D.; Raróg-Pilecka, W. Surface enrichment phenomenon in the Ba-doped cobalt catalyst for ammonia synthesis. *Vacuum* **2019**, *168*, 108831. [[CrossRef](#)]
118. Menon, P.G.; Rao, T.S.R.P.; Prasad Rao, T.S.R.R. Surface Enrichment in Catalysts. *Catal. Rev.* **1979**, *20*, 97–120. [[CrossRef](#)]

119. Karolewska, M.; Truszkiewicz, E.; Mierzwa, B.; Kępiński, L.; Raróg-Pilecka, W. Ammonia synthesis over cobalt catalysts doped with cerium and barium. Effect of the ceria loading. *Appl. Catal. A Gen.* **2012**, *445–446*, 280–286. [[CrossRef](#)]
120. Tarka, A.; Zybert, M.; Kindler, Z.; Szmurło, J.; Mierzwa, B.; Raróg-Pilecka, W. Effect of precipitating agent on the properties of cobalt catalysts promoted with cerium and barium for NH<sub>3</sub> synthesis obtained by co-precipitation. *Appl. Catal. A Gen.* **2017**, *532*, 19–25. [[CrossRef](#)]
121. Tarka, A.; Patkowski, W.; Zybert, M.; Ronduda, H.; Wiciński, P.; Adamski, P.; Sarnecki, A.; Moszyński, D.; Raróg-Pilecka, W. Synergistic interaction of cerium and barium—new insight into the promotion effect in cobalt systems for ammonia synthesis. *Catalysts* **2020**, *10*, 658. [[CrossRef](#)]
122. Li, W.; Wang, S.; Li, J. Highly Effective Ru/BaCeO<sub>3</sub> Catalysts on Supports with Strong Basic Sites for Ammonia Synthesis. *Chem. Asian J.* **2019**, *14*, 2815–2821. [[CrossRef](#)] [[PubMed](#)]
123. Wang, Z.; Liu, B.; Lin, J. Highly effective perovskite-type BaZrO<sub>3</sub> supported Ru catalyst for ammonia synthesis. *Appl. Catal. A Gen.* **2013**, *458*, 130–136. [[CrossRef](#)]
124. Ahmadi, S.; Kaghazchi, P. On the origin of high activity of hcp metals for ammonia synthesis. *Phys. Chem. Chem. Phys.* **2016**, *18*, 5291–5298. [[CrossRef](#)]
125. Zhang, B.-Y.; Chen, P.-P.; Liu, J.-X.; Su, H.-Y.; Li, W.-X. Influence of Cobalt Crystal Structures on Activation of Nitrogen Molecule: A First-Principles Study. *J. Phys. Chem. C* **2019**, *123*, 10956–10966. [[CrossRef](#)]
126. Tarka, A.; Zybert, M.; Ronduda, H.; Patkowski, W.; Mierzwa, B.; Kępiński, L.; Raróg-Pilecka, W. On Optimal Barium Promoter Content in a Cobalt Catalyst for Ammonia Synthesis. *Catalysts* **2022**, *12*, 199. [[CrossRef](#)]
127. Patkowski, W.; Kowalik, P.; Antoniuk-Jurak, K.; Zybert, M.; Ronduda, H.; Mierzwa, B.; Próchniak, W.; Raróg-Pilecka, W. On the Effect of Flash Calcination Method on the Characteristics of Cobalt Catalysts for Ammonia Synthesis Process. *Eur. J. Inorg. Chem.* **2021**, *2021*, 1518–1529. [[CrossRef](#)]
128. Lin, B.; Qi, Y.; Wei, K.; Lin, J. Effect of pretreatment on ceria-supported cobalt catalyst for ammonia synthesis. *RSC Adv.* **2014**, *4*, 38093. [[CrossRef](#)]
129. Chen, B.; Ma, Y.; Ding, L.; Xu, L.; Wu, Z.; Yuan, Q.; Huang, W. Reactivity of hydroxyls and water on a CeO<sub>2</sub>(111) thin film surface: The role of oxygen vacancy. *J. Phys. Chem. C* **2013**, *117*, 5800–5810. [[CrossRef](#)]
130. Lin, B.; Liu, Y.; Heng, L.; Ni, J.; Lin, J.; Jiang, L. Effect of ceria morphology on the catalytic activity of Co/CeO<sub>2</sub> catalyst for ammonia synthesis. *Catal. Commun.* **2017**, *101*, 15–19. [[CrossRef](#)]
131. Wang, X.; Li, L.; Zhang, T.; Lin, B.; Ni, J.; Au, C.-T.; Jiang, L. Strong metal-support interactions of Co-based catalysts facilitated by dopamine for highly efficient ammonia synthesis: In situ XPS and XAFS spectroscopy coupled with TPD studies. *Chem. Commun.* **2019**, *55*, 474–477. [[CrossRef](#)] [[PubMed](#)]
132. Lin, B.; Liu, Y.; Heng, L.; Lin, J.; Ni, J.; Jiang, L. Cobalt-Based Ammonia Synthesis Catalyst with Cerium Oxide as Carrier and Preparation Method of Cobalt-Based Ammonia Synthesis Catalyst. CN107008335A, 4 August 2017.
133. Ni, J.; Zhou, L.; Lin, B.; Lin, J.; Jiang, L. Cerium Oxide-Loaded High-Surface-Defect Cobalt Oxide Ammonia Synthesis Catalyst. CN113181926A, 30 July 2021.
134. Zybert, M.; Karasińska, M.; Truszkiewicz, E.; Mierzwa, B.; Raróg-Pilecka, W. Properties and activity of the cobalt catalysts for NH<sub>3</sub> synthesis obtained by co-precipitation—The effect of lanthanum addition. *Pol. J. Chem. Technol.* **2015**, *17*, 138–143. [[CrossRef](#)]
135. Zybert, M.; Tarka, A.; Mierzwa, B.; Kępiński, L.; Raróg-Pilecka, W. Promotion effect of lanthanum on the Co/La/Ba ammonia synthesis catalysts—The influence of lanthanum content. *Appl. Catal. A Gen.* **2016**, *515*, 16–24. [[CrossRef](#)]
136. Ronduda, H.; Zybert, M.; Patkowski, W.; Ostrowski, A.; Jodłowski, P.; Szymański, D.; Kępiński, L.; Raróg-Pilecka, W. Development of cobalt catalyst supported on MgO-Ln<sub>2</sub>O<sub>3</sub> (Ln = La, Nd, Eu) mixed oxide systems for ammonia synthesis. *Int. J. Hydrogen Energy* **2022**, *47*, 6666–6678. [[CrossRef](#)]
137. Ronduda, H.; Zybert, M.; Patkowski, W.; Ostrowski, A.; Jodłowski, P.; Szymański, D.; Raróg-Pilecka, W. Co supported on Mg-La mixed oxides as an efficient catalyst for ammonia synthesis. *Int. J. Hydrogen Energy* **2022**, *47*, 35689–35700. [[CrossRef](#)]
138. Ronduda, H.; Zybert, M.; Dziewulska, A.; Patkowski, W.; Sobczak, K.; Ostrowski, A.; Raróg-Pilecka, W. Ammonia synthesis using Co catalysts supported on MgO-Nd<sub>2</sub>O<sub>3</sub> mixed oxide systems: Effect of support composition. *Surf. Interfaces* **2023**, *36*, 102530. [[CrossRef](#)]
139. Ronduda, H.; Zybert, M.; Patkowski, W.; Tarka, A.; Jodłowski, P.; Kępiński, L.; Sarnecki, A.; Moszyński, D.; Raróg-Pilecka, W. Tuning the catalytic performance of Co/Mg-La system for ammonia synthesis via the active phase precursor introduction method. *Appl. Catal. A Gen.* **2020**, *598*, 117553. [[CrossRef](#)]
140. Ronduda, H.; Zybert, M.; Patkowski, W.; Sobczak, K.; Moszyński, D.; Albrecht, A.; Sarnecki, A.; Raróg-Pilecka, W. On the effect of metal loading on the performance of Co catalysts supported on mixed MgO-La<sub>2</sub>O<sub>3</sub> oxides for ammonia synthesis. *RSC Adv.* **2022**, *12*, 33876–33888. [[CrossRef](#)] [[PubMed](#)]
141. Ronduda, H.; Zybert, M.; Patkowski, W.; Moszyński, D.; Albrecht, A.; Sobczak, K.; Małolepszy, A.; Raróg-Pilecka, W. Co nanoparticles supported on mixed magnesium–lanthanum oxides: Effect of calcium and barium addition on ammonia synthesis catalyst performance. *RSC Adv.* **2023**, *13*, 4787–4802. [[CrossRef](#)] [[PubMed](#)]
142. Ronduda, H.; Zybert, M.; Patkowski, W.; Tarka, A.; Ostrowski, A.; Raróg-Pilecka, W. Kinetic studies of ammonia synthesis over a barium-promoted cobalt catalyst supported on magnesium–lanthanum mixed oxide. *J. Taiwan Inst. Chem. Eng.* **2020**, *114*, 241–248. [[CrossRef](#)]

143. Ronduda, H.; Zybert, M.; Patkowski, W.; Ostrowski, A.; Jodłowski, P.; Szymański, D.; Kępiński, L.; Raróg-Pilecka, W. Boosting the Catalytic Performance of Co/Mg/La Catalyst for Ammonia Synthesis by Selecting a Pre-Treatment Method. *Catalysts* **2021**, *11*, 941. [[CrossRef](#)]
144. Ronduda, H.; Zybert, M.; Patkowski, W.; Ostrowski, A.; Jodłowski, P.; Szymański, D.; Kępiński, L.; Raróg-Pilecka, W. A high performance barium-promoted cobalt catalyst supported on magnesium-lanthanum mixed oxide for ammonia synthesis. *RSC Adv.* **2021**, *11*, 14218–14228. [[CrossRef](#)]
145. Zybert, M.; Tarka, A.; Patkowski, W.; Ronduda, H.; Mierzwa, B.; Kępiński, L.; Raróg-Pilecka, W. Structure Sensitivity of Ammonia Synthesis on Cobalt: Effect of the Cobalt Particle Size on the Activity of Promoted Cobalt Catalysts Supported on Carbon. *Catalysts* **2022**, *12*, 1285. [[CrossRef](#)]
146. Patkowski, W.; Zybert, M.; Ronduda, H.; Gawrońska, G.; Albrecht, A.; Moszyński, D.; Fidler, A.; Dłużewski, P.; Raróg-Pilecka, W. The Influence of Active Phase Content on Properties and Activity of Nd<sub>2</sub>O<sub>3</sub>-Supported Cobalt Catalysts for Ammonia Synthesis. *Catalysts* **2023**, *13*, 405. [[CrossRef](#)]
147. Liu, J.-X.; Li, W.-X. Theoretical study of crystal phase effect in heterogeneous catalysis. *Wiley Interdiscip. Rev. Comput. Mol. Sci.* **2016**, *6*, 571–583. [[CrossRef](#)]
148. Weststrate, C.J.; Mahmoodinia, M.; Farstad, M.H.; Svenum, I.-H.; Strømsheim, M.D.; Niemantsverdriet, J.W.; Venvik, H.J. Interaction of hydrogen with flat (0001) and corrugated (11–20) and (10–12) cobalt surfaces: Insights from experiment and theory. *Catal. Today* **2020**, *342*, 124–130. [[CrossRef](#)]
149. Weststrate, C.J.; Rodriguez, D.G.; Sharma, D.; (Hans) Niemantsverdriet, J.W. Structure-dependent adsorption and desorption of hydrogen on FCC and HCP cobalt surfaces. *J. Catal.* **2022**, *405*, 303–312. [[CrossRef](#)]
150. Ogawa, T.; Masaki, Y.; Keiichi, I. Techno-economic analysis on recent heterogeneous catalysts for ammonia synthesis. *ChemRxiv* **2022**. [[CrossRef](#)]
151. Mayer, P.; Ramirez, A.; Pezzella, G.; Winter, B.; Sarathy, S.M.; Gascon, J.; Bardow, A. Blue and green ammonia production: A techno-economic and life cycle assessment perspective. *iScience* **2023**, *26*, 107389. [[CrossRef](#)] [[PubMed](#)]
152. Park, S.; Shin, Y.; Jeong, E.; Han, M. Techno-economic analysis of green and blue hybrid processes for ammonia production. *Korean J. Chem. Eng.* **2023**, *40*, 2657–2670. [[CrossRef](#)]
153. Alvero, R.; Odriozola, J.A.; Trillo, J.M.; Bernal, S. Lanthanide oxides: Preparation and ageing. *J. Chem. Soc. Dalt. Trans.* **1984**, *2*, 87. [[CrossRef](#)]
154. Alvero, R.; Bernal, A.; Carrizosa, I.; Odriozola, J.A.; Trillo, J.M. The kinetics of Ln<sub>2</sub>O<sub>3</sub> Hydration under mild conditions. *J. Therm. Anal.* **1987**, *32*, 637–643. [[CrossRef](#)]
155. Bernal, S.; Blanco, G.; Calvino, J.J.; Omil, J.A.P.; Pintado, J.M. Some major aspects of the chemical behavior of rare earth oxides: An overview. *J. Alloys Compd.* **2006**, *408–412*, 496–502. [[CrossRef](#)]

**Disclaimer/Publisher's Note:** The statements, opinions and data contained in all publications are solely those of the individual author(s) and contributor(s) and not of MDPI and/or the editor(s). MDPI and/or the editor(s) disclaim responsibility for any injury to people or property resulting from any ideas, methods, instructions or products referred to in the content.